Title

Transcriptional Regulation of Early Adenovirus Genes by Adenovirus Large E1A via Interactions with p300

Permalink

https://escholarship.org/uc/item/4pb9h4r2

Author

Hsu, Emily

Publication Date

2020

Peer reviewed|Thesis/dissertation

UNVERSITY OF CALIFORNIA

Los Angeles

Transcriptional Regulation of Early Adenovirus Genes

by Adenovirus Large E1A via Interactions with p300

A dissertation submitted in partial satisfaction of the requirements for

the degree of Doctor of Philosophy in Molecular Biology

by

Emily Hsu

2020

ABSTRACT OF THE DISSERTATION

Transcriptional Regulation of Early Adenovirus Genes

by Adenovirus Large E1A via Interactions with p300

by

Emily Hsu

Doctor of Philosophy in Molecular Biology

University of California, Los Angeles, 2020

Professor Arnold J. Berk, Chair

The human adenovirus early region 1A (E1A) has been extensively studied as a model transcriptional regulator to uncover the molecular mechanisms that regulate viral and cellular gene expression. While it was initially thought that early viral gene activation by E1A was primarily due to association of CR3 with Mediator, it was recently demonstrated by Pelka et al. that an interaction between HATs p300/CBP and a region of E1A including CR3 also stimulates transcription (1). To further analyze this mechanism, we assayed the association of YFP labeled p300 with truncated E1A proteins fused to mCherry labeled LacI bound to a LacO array in nuclei. Either of two highly acidic regions flanking CR3 were identified as being required for E1A association with p300 in vivo. Infection of primary human airway epithelial cells with Ad recombinants expressing alanine substitutions in both acidic regions resulted in greatly decreased expression of E2 and E4 RNAs. ChIP-seq for H3K18/27ac and Pol2 pre-initiation complex (PIC)

components revealed decreased levels of H3 acetylation at the E2early, E3, and E4 promoters and defective TBP and Pol2 assembly at the E2early promoter after infection with the Ad mutant. GRO-seq in infected cells demonstrated decreased release of promoter-proximal paused Pol2 at E4 by p300 binding mutant E1A. Our results demonstrate that transcription of E2early is regulated during Pol2 PIC assembly mediated by H3 acetylation and E4 is regulated during the transition to productive transcriptional elongation, both of which are dependent on the presence of these acidic regions of E1A.

The dissertation of Emily Hsu is approved.

Douglas L. Black

Michael F. Carey

Siavash K. Kurdistani

Stephen Smale

Arnold J. Berk, Committee Chair

University of California, Los Angeles

2020

DEDICATION

This dissertation is dedicated to my family- Mom, Dad, Justin, and Esther, for their unwavering love and support; to my mentor Dr. Arnold Berk, for his guidance, encouragement, and for imparting his excitement for scientific discovery; to my committee members for their helpful advice and discussions; to Berk lab members for creating a lab space that I truly enjoyed and will sincerely miss; and to my friends, for all the fun times.

TABLE OF CONTENTS

LIST OF FIGURES

'

LIST OF TABLES

ACKNOWLEDGEMENTS

<div align="center">**VITA**</div>

EDUCATION

New York University   New York, NY

B.A.   2012

PUBLICATIONS

Hsu E, Pennella MA, Zemke NR, Eng C, Berk AJ. 2018. Adenovirus E1A activation domain regulates H3 acetylation affecting varied steps in transcription at different viral promoters. Journal of Virology 92:e00805-18. https://doi.org/10.1128/JVI.00805-18.

Yotova I, **Hsu E**, Do C, Gaba A, Sczabolcs M, Dekan S, Kenner L, Wenzl R, Tycko B. 2017. Epigenetic Alterations Affecting Transcription Factors and Signaling Pathways in Stromal Cells of Endometriosis. PLoS ONE 12(1): e0170859. doi: 10.1371/journal.pone.0170859.

PRESENTATIONS

Hsu E, Pennella MA, Zemke NR, Eng C, Berk AJ. Transcriptional Regulation of Early Adenovirus Promoters by Large E1A via Interactions with p300. Cold Spring Harbor Laboratory Mechanisms of Eukaryotic Transcription Meeting. Cold Spring Harbor, NY, August 2019. (Poster presentation)

Hsu E, Pennella MA, Zemke NR, Eng C, Berk AJ. Transcriptional Activation of Early Viral Promoters by Adenovirus Large E1A via Interactions with p300. DNA Tumor Virus Meeting. Birmingham, UK, July 2017. (Oral presentation)

Hsu E, Pennella MA, Zemke NR, Eng C, Berk AJ. Transcriptional Activation of Early Viral Promoters by Adenovirus Large E1A via Interactions with p300. UCLA Jonsson Comprehensive Cancer Center Gene Regulation Intramural Group Meeting. June 2017. (Oral presentation)

Chapter 1: INTRODUCTION

Proteins encoded in early region 1A (E1A) of human adenoviruses (Ad) have been studied extensively as model transcriptional regulators to uncover molecular mechanisms that control viral and cellular gene expression. Upon infection, E1A is the first viral region transcribed, and E1A pre-mRNA is alternatively spliced into mRNAs, designated 13S, 12S, and 9S mRNAs, as well as the less abundant 10S and 11S mRNAs (2). The 13S and 12S transcripts are generated from two 5′ splice sites, separated by 138 bp and a common 3′ splice site, and are most abundant early after infection and in transformed cells. They encode the 289-amino-acid (aa) large E1A and the 243-aa small e1a proteins, respectively (3). E1A proteins do not bind directly to DNA and exert their considerable effects on gene expression by interacting with cellular proteins through sequences conserved throughout primate adenovirus species and serotypes, designated conserved regions 1 to 4 (CR1-CR4) (4, 5) (Figure 1-1).

Large and small E1A both contain the N-terminal CR1 and CR2, which interact with the closely related nuclear lysine acetyltransferases CBP/p300 and RB family proteins (RB1, p107, and p130) to reprogram host cell gene expression and induce S phase in quiescent host cells (6, 7) (Figure 1-1) The small e1a N-terminal ~12 aa and aa 54 to 82 of CR1 bind the TAZ2 domain of CBP/p300 (8). p300/CBP is primarily responsible for mediating the acetylation of histone H3 at lysines 18 (H3K18) and 27 (H3K27), which are generally associated with promoters of actively transcribed regions (9, 10). The association of p300/CBP with small e1a inhibits H3K18/27 acetylation to about 30% the level in uninfected cells (6). This is thought to be the primary mechanism by which adenovirus represses host cell genes that would otherwise interfere with productive viral infection (6, 9).

While small e1a has been well characterized in the context described above, large E1A is known to modulate viral infection additionally by activating transcription from early adenovirus

promoters E1A and E1B and, to a greater extent, E2early, E3, and E4 (11–14). Large E1A is primarily responsible for transcriptional activation from these promoters. Although small e1a is a much weaker activator of these promoters than large E1A, small e1a does activate transcription significantly compared to that of the E1A deletion mutant *dl*312 (14). The E1A activation domain includes CR3 [E1A(aa 140–185)], a region that is unique to large E1A. When fused to the GAL4 DNA-binding domain (DBD), E1A(aa 121–223), including CR3, functions as a strong activation domain (15). Further studies using Gal4-DBD fusions to progressive N- and C-terminal deletions of E1A(aa 121–223) suggested that the minimal region required for activation is aa 141 to 178, closely overlapping CR3 (16). Six tandem glutamic acid-proline repeats (EP$_6$) just C terminal to CR3 (aa 189 to 200; designated AR1) were later shown to be essential for activation of early viral promoters by native E1A (not fused to the Gal4-DBD) in transient-transfection assays (17, 18).

In an early model of the mechanism of E1A activation of early viral promoters, the E1A activation domain was functionally divided into two distinct subdomains: a C$_4$ Zn-finger region that makes contact with the basal transcriptional machinery and a C-terminal region (aa 183 to 188) implicated in promoter binding via association with host cell sequence-specific transcription factors (15, 16, 19, 20). Importantly, the large E1A activation domain, E1A(aa 121–123), binds human multisubunit mediator complexes, key coactivators required for regulating transcription by RNA polymerase II (Pol II) (21, 22). Affinity columns of E1A(aa 121–223) and amino acid substitution mutants that activate transcription were found to bind directly to the human homolog of *Caenorhabditis elegans* Sur2, now designated MED23, a mediator subunit located in the tail domain of the human mediator complex (23). Mutant E1As with amino acid substitutions in the C$_4$ Zn-finger region (Figure 1-1) that are defective for activation (19) did not

bind MED23, demonstrating that MED23 associates with the Zn-finger subdomain of CR3 (21). Further work confirmed this CR3-MED23 interaction *in vivo* (24) and demonstrated its ability to stimulate Pol II preinitiation complex (PIC) assembly on promoter DNA *in vitro* (25).

While it was initially thought that activation by E1A was primarily due to its association with the mediator complex, Pelka et al. proposed that an additional E1A interaction with p300/CBP also contributes to E1A activation (1). This group reported that transcriptional activation by E1A(aa 139–204) was inhibited by overexpression of small e1a, dependent on the interaction of small e1a with p300/CBP. This result was interpreted to indicate that small e1a antagonizes transcriptional activation by large E1A through its well-characterized binding to the CBP/p300 TAZ2 domain via the E1A N terminus and CR1 (8). Further, p300/CBP also was observed to bind E1A(aa 139–204), although it did so more weakly than the well-characterized sites of E1A interaction at the N terminus and CR1 (1).

In this work, we confirm the second interaction between p300 and E1A proposed by Pelka et al., and map it to two highly acidic peptide regions flanking CR3. We also present a model where H3 acetylation mediated by this interaction affects early viral promoters at different steps in transcription.
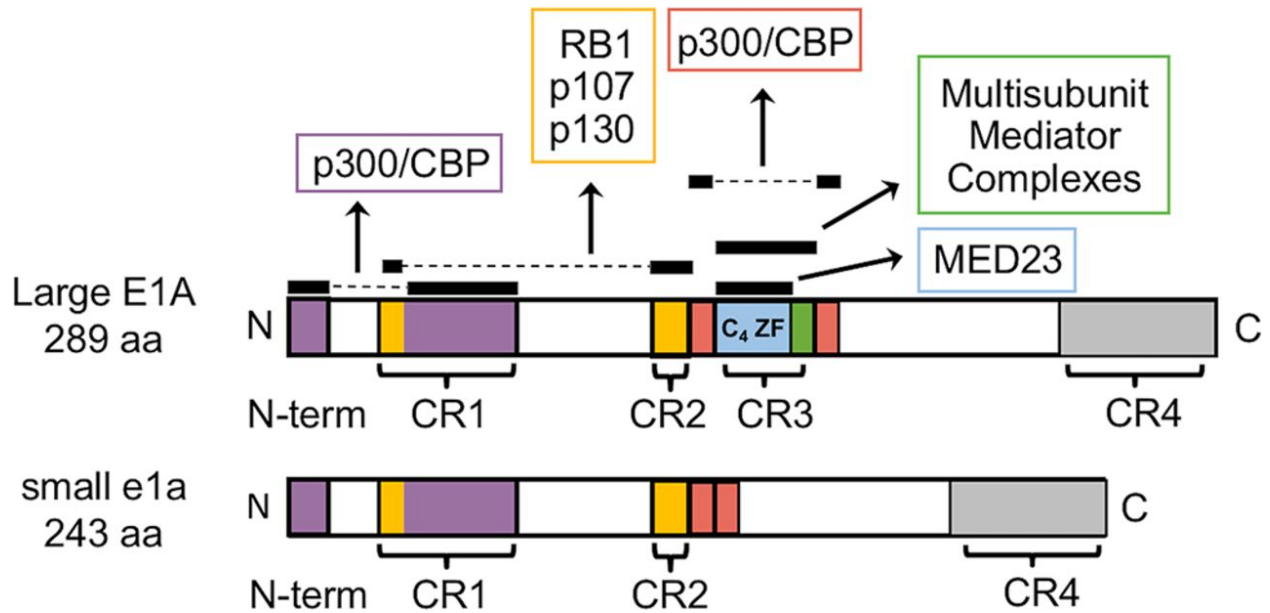
Figure 1-1: Small and large E1A protein interactions

Small and large E1A protein interactions. E1A interaction maps for large E1A (289 aa) and small e1a (243 aa). Colored portions and horizontal black bars above them represent regions of E1A that interact with the cellular protein indicated by the associated arrowhead pointing to a box containing the name of the cellular protein. Dashed lines connect conserved regions of E1A that bind the indicated targets together. Conserved regions (CR) 1 to 4 are indicated in brackets. Results presented below indicate that the red regions interact with p300 and that the green region at the C-terminal end of CR3 is required for binding multisubunit mediator complexes.

Chapter 2: ADENOVIRUS E1A ACTIVATION DOMAIN REGULATES H3 ACETYLATION AFFECTING VARIED STEPS IN TRANSCRIPTION AT DIFFERENT VIRAL PROMOTERS

Introduction

To corroborate the conclusions of Pelka et al. by an independent method, we analyzed

p300 interaction with E1A(aa 121–223) *in vivo* by confocal microscopy of green fluorescent

protein (GFP)-derivative tagged proteins. We constructed Ad mutants with multialanine

substitutions in E1A regions observed to be required for the interaction with p300 in this *in*

vivo protein-protein interaction assay and analyzed transcription from early viral promoters after

infection of human primary airway epithelial cells. Additionally, we used these same methods to

further characterize the association of multisubunit mediator complexes with the E1A activation

domain and propose a new explanation for the requirement of the CR3 C-terminal invariant

region (aa 183 to 188) for activation. Using chromatin immunoprecipitation sequencing (ChIP-

seq), we analyzed the association of modified histones, TBP, and Pol II with the early viral

promoters after infection with wild-type (wt) and Ad5 mutants. We found that eliminating the

interaction between the large E1A activation domain and p300 prevented H3K18/27ac at the

adenovirus E2early, E3, and E4 promoters during the early phase of infection. The consequences

of this failure to acetylate H3K18/27 in these promoter regions for PIC assembly and

transcription were different at each of these viral promoters.

Results

Acidic regions flanking E1A CR3 are required for p300 binding to the E1A activation domain,

and amino acids 179 to 189 are required for E1A binding to multisubunit mediator complexes in

vivo.

Pelka et al. reported that p300 interacts with large E1A(aa 139–204), a region lacking the

well-characterized large and small E1A p300/CBP binding site formed from the E1A N-terminal

~12 aa plus E1A(aa 54–82) in CR1 (1, 8). To confirm and extend this conclusion, we analyzed

protein-protein interactions *in vivo* by confocal fluorescence microscopy of proteins fused to

differently colored GFP derivatives. Expression vectors for YFP-p300 and LacI-mCherry alone

or LacI-mCherry fused to an E1A fragment consisting of aa 121 to 223, E1A(aa 121–223), were

transfected into CHO-A03.1 cells. These cells contain an amplified region of DNA with

~10,000 *lac* operator sites (*lacO*) integrated into a single region of one chromosome (26).

Expression of mCherry-tagged Lac repressor (LacI-mCherry) resulted in clear association of this

fusion protein with the *lacO* array, as observed by a localized nuclear mCherry signal (Figures 2-

1b, 2-1c). Coexpressed YFP-p300 did not colocalize with LacI-mCherry at the *lacO* array

(Figures 2-1a – 2-1c) However, when coexpressed with LacI-mCherry-E1A(121–223), YFP-

p300 did colocalize with the *lacO* array (Figures 2-1d – 2-1f), confirming the interaction of

E1A(aa 121–223) with p300 *in vivo* (1).

    To identify the amino acids of large E1A required for this specific association with p300,

we assayed colocalization of YFP-p300 with LacI-mCherry fused to deletions of E1A(aa 121–

223) (Figure 2-2a). Fusion proteins that retained either one of two highly acidic peptides flanking

CR3, aa 133 to 138 (DDEDEE) or aa 189 to 200 (EPEPEPEPEPEP) (red in Figures 2-2a and 2-

2f), continued to colocalize with YFP-p300, but E1A(aa 140–189) and E1A(aa 140–178), which

have both acidic peptides deleted, did not (Figure 2-2e) and Table 2-1). These results suggest

that both acidic regions flanking CR3 contribute to p300 binding and that at least one of these

acidic regions is required for p300 binding to the E1A activation domain, as detected in this *in

vivo* colocalization assay.

    We further characterized the known association of E1A and mediator complexes. *In

vivo* colocalization, assayed as described above, was again used to observe the association of

E1A deletion constructs with mediator subunit MED23, located in the tail of the mediator (23) and bound directly by large E1A (21), and MED6, located in the head domain of the mediator (23) (Figure 2-1g – 2-1i). We interpreted colocalization of an E1A fragment with YFP-MED6 to indicate that multisubunit mediator complexes associate with the fragment. Consistent with previous results, E1A(aa 121–223) associated with MED23 (21, 27). However, in contrast to E1A(aa 121–223), the E1A C4 Zn-finger region alone (aa 140 to 178) (28) associated with MED23 but was greatly reduced in its association with MED6, as was E1A(aa 133–178) (Figure 2-2c, 2-2d and Table 2-1). Interestingly, binding of both MED23 and MED6 required aa 140 to 189 (Figure 2-2c, 2-2d and Table 2-1). These results indicate that E1A(aa 140–178) interacts with MED23, while the additional residues 179 to 189 (green in Figure 1-1 and Figure 2-2a) are required to bind multisubunit mediator complexes containing the assayed MED6 head subunit.
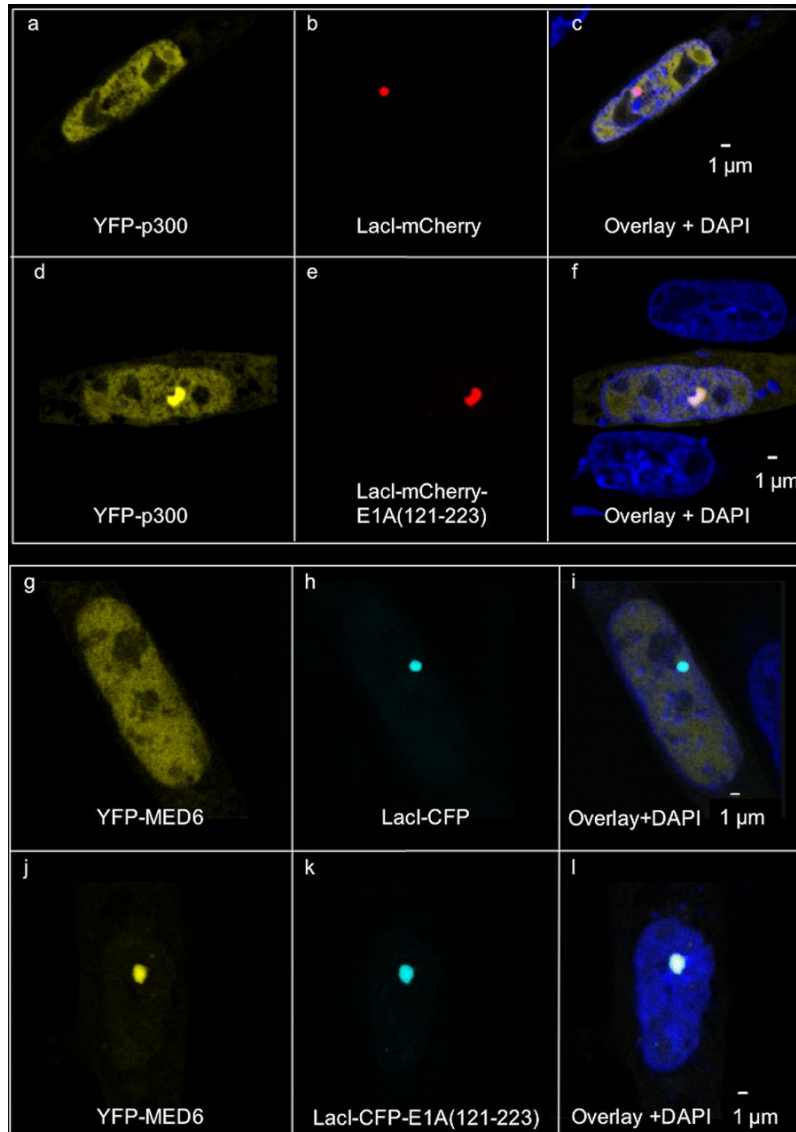
Figure 2-1: In vivo colocalization assays for association of fragments of large E1A with p300 and MED6.

(Upper) Confocal micrographs of YFP and mCherry fluorescence in CHO-A03.1 cells cotransfected with expression vectors for YFP-p300 and LacI-mCherry (a to c) or YFP-p300 and LacI-mCherry-E1A(121–223) (d to f).

(Lower) As described for upper images but with expression vectors for YFP-MED6 and LacI-CFP (g to i) or YFP-MED6 and LacI-CFP-E1A(121–223) (j to l).

Labeled protein	Colocalization score (%; no. of cells scored) for indicated E1A fragment fused to tagged LacI[a]:							
	LacI	121–223	133–178	133–189	133–205	140–178	140–189	140–205
YFP-MED6	5; 22	79; 24	30; 27	80; 20	70; 20	26; 35	84; 25	76; 25
YFP-MED23	23; 30	100; 14	ND	ND	ND	100; 15	ND	ND
YFP-p300	0; 21	86; 21	64; 21	86; 15	73; 20	3; 23	4; 22	64; 20

↵a ND, not done.

Table 2-1: Colocalization score of LacI-mCherry or LacI-mCherry-E1A fragment with YFP-MED6, YFP-MED23, or YFP-p300.
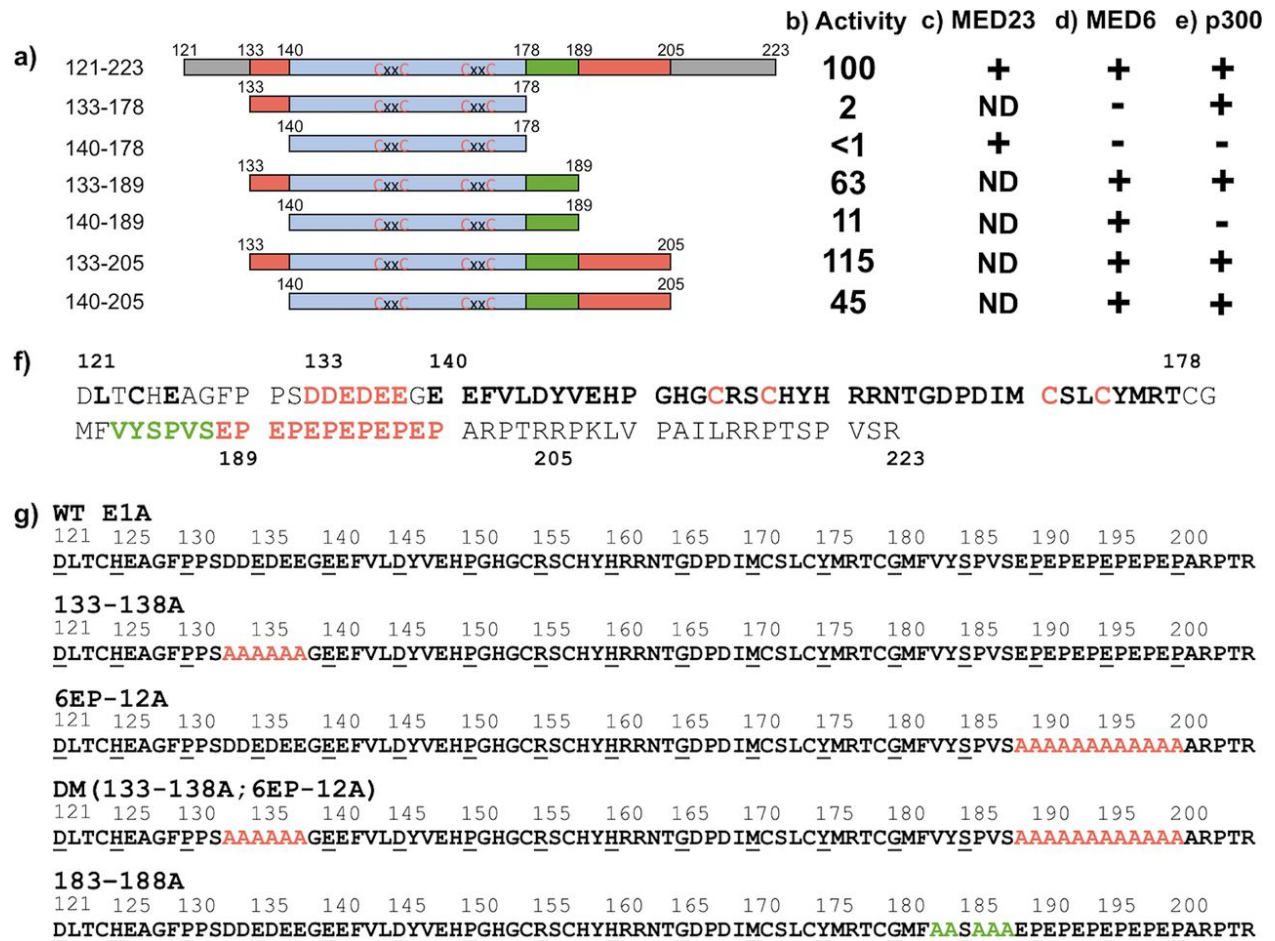
Figure 2-2: Summary of E1A deletion constructs and Ad5 mutant sequences.

(a) Diagram of E1A regions fused to LacI used for colocalization and transient-transfection activation assays. E1A(aa 133–139) and E1A(aa 190–205) containing acidic peptides are shown in red. E1A(aa 179–189) is shown in green. The C4 Zn-finger region (aa 140 to 178) is shown in light blue, with cysteines shown in red.

(b) Activation by LacI-mCherry fusions to E1A fragments in a transient-transfection luciferase reporter assay in CHO cells. The luciferase reporter had eight *lacO* sites upstream of the E1B promoter. Values are relative (rel.) to activity of LacI-mCherry-E1A(121–223).

(c) Colocalization of LacI-CFP-E1A fragments with YFP-MED23. ND (not done) indicates E1A fragments that were not assayed for colocalization.

(d) Colocalization of LacI-CFP-E1A fragments with YFP-MED6.

(e) Colocalization of LacI-mCherry-E1A fragments with YFP-p300.

(f) The amino acid sequence of wt Ad5 E1A(121–223). The LxCxE motif of CR2 (aa 122 to 126) is in boldface. Acidic peptide sequences (aa 133 to 138, DDEDEE, and aa 189 to 200, EPEPEPEPEPEP) are shown in red. The invariant sequence in the interval E1A(aa 183–188) is in green. The C4 Zn-finger region (aa 140 to 178) is in boldface, with cysteines in red.

(g) Sequences of Ad5 mutants from E1A(aa 121–223), with alanine substitutions in red or green.

Both p300 and multisubunit mediator binding by E1A are necessary for high levels of activation in a transient-transfection assay.

Several groups previously have defined the boundaries of the CR3 activation domain using transient-transfection reporter assays. E1A(aa 140–178), including a C4-type zinc finger, is essential for activation (15, 16, 19). In addition, peptide regions that closely overlap those that we propose to contribute to p300 and multisubunit mediator binding (aa 190 to 205 and aa 179 to 189, respectively) are required for high levels of activation (17–19). To determine if activation by the LacI-mCherry-truncated E1A fragments analyzed here is consistent with previously demonstrated activation by E1A fragments in transient-transfection assays, we assayed activation by these LacI fusions using a luciferase reporter with eight *lacO* sites upstream of the E1B promoter (Figure 2-2b)(29). These assays were done in CHO-K1 cells, the parental cells for the A03.1 cells used in the colocalization assays.

Although deletion of either the N- or C-terminal acidic region of E1A(aa 133–205) did not affect p300 binding in our *in vivo* colocalization assay, E1A(aa 133–189) and E1A(aa 140–205), each lacking one of the two acidic peptides flanking CR3, displayed partial defects in activation, with ∼50% of the activity of E1A(aa 121–223) (Figure 2-2b). Deletion of both acidic regions and the consequential complete loss of p300 binding by this region of E1A(aa 140–189) (Figure 2-2e and Table 1)resulted in a much greater defect in activation, with only ∼10% the activity of E1A(aa 121–223) (Figure 2-2b). The greatest defect in activation resulted from loss of association with multisubunit mediator complexes. E1A(aa 133–178) and E1A(aa 140–178), both lacking aa 179 to 189, had <3% the activity of E1A(aa 121–223), regardless of their ability to associate with p300 (Figure 2-2b – 2-2e). These results indicate that E1A binding to a multisubunit mediator complex is essential for activation by E1A(aa 121–223), and that the

additional interaction with p300 further stimulates transcription ~10-fold in this transient-transfection assay.

During adenovirus infection, transcription from each of the viral early promoters responds differently to multialanine substitutions in subdomains of the E1A activation domain.

To determine whether the decreased activation by LacI-E1A deletions in transient-transfection assays is recapitulated by comparable E1A mutants during adenovirus infection, we constructed Ad5 mutants with multialanine substitutions in E1A regions necessary for maximal activation in the transient-transfection assay (Figure 2-2g). These included the 133–138A and 6EP–12A mutants, with alanine substitutions in the N- and C-terminal acidic regions (Figures 2-2a and 2-2g, red regions), respectively, the double mutant (DM), with alanine substitutions in both acidic regions, and the 183 to 188A mutant, with alanine substitutions in the invariant region required for binding multisubunit mediator complexes (Figures 2-2a and 2-2g, green regions). Alanine substitutions in both acidic regions or the invariant region (183–188A mutant) did not interfere with E1A pre-mRNA splicing (Figure 2-3a). Note that as a result of their construction by *in vivo* Cre-mediated site-specific recombination with the Ψ5 vector (30), all of these E1A mutants and control wild-type (wt) E1A were expressed from viral genomes that also contain an inactivating insertion of a *loxP* site in the C-terminal region of the E1B-55K coding region and a deletion of most of E3.

Viral promoter activation was assayed during infection of primary human bronchial/tracheal epithelial cells (HBTECs), derived from the natural Ad5 host tissue. We first analyzed the consequences of mutations in the DM, since deletion of both of the mutated regions in the DM was required to eliminate the interaction of E1A with p300 in the *in*

vivo colocalization assay. HBTECs grown to confluence and arrested in G1 were infected with

Ad5 mutants expressing either wt or mutant E1As. When infected at equal multiplicities of

infection (MOIs) of 20, we observed that HBTECs expressed considerably more wt than DM

E1A protein (data not shown), possibly due to differences in protein stability caused by the

introduced mutations. Therefore, in order to achieve equal levels of wt and DM E1A protein,

cells were infected with the wt virus at an MOI of 5 and diluted with the E1A deletion

mutant *dl*312 at an MOI of 95. Alternatively, cells were infected with the DM virus alone at an

MOI of 100. Under these conditions, the levels of wt and mutant E1A proteins were similar at 12

and 18 h postinfection (p.i.) (Figure 2-3b). Further, dilution of the wt virus with dl312 gives the

same concentration of adenovirus DNA template for all viral genes other than E1A compared to

infections with the DM virus alone. Total RNA was isolated during the early phase of infection

at 6, 12, and 18 h p.i. The late phase, determined by the onset of viral DNA replication, begins

~24 h p.i. in these cells (data not shown). Viral RNAs transcribed from the early promoters

E2early, E3, and E4, as well as late region L3 RNA, including hexon mRNA, were quantified by

qRT-PCR (Figure 2-3c). An unanticipated and remarkable result from these assays is that

transcription from the different viral early promoters responded differently to the DM E1A

multialanine substitutions.

Dramatic decreases in expression by the E1A DM were observed for RNAs transcribed

from the E2 and E4 promoters, especially at 12 h p.i. (Figure 2-3c). In contrast, no significant

decrease in E3 RNA expression was observed at 12 h p.i., and only a modest (~50%) decrease

was observed at 18 h p.i. (Figure 2-3c). The very low level of L3 RNA in the DM-expressing

cells was similar in the coinfection of wt E1A and *dl*312 viruses at 12 h p.i. and was only very

modestly decreased at 18 h p.i. While E2, E3, and L3 RNA increased between 12 h and 18 h p.i.

in response to wt E1A, E4 RNA nearly reached a plateau at 12 h (Figure 2-3c). This may be due to a decrease in the rate of E4 transcription between 12 and 18 h p.i., to changes in the stability of E4 RNA, or both.

Interpretation of expression levels for E1A and E1B are complicated by the 20-fold higher E1A template concentration in the DM-infected cells than the coinfection. *dl*312 is deleted for sequences from −50 relative to the major E1A transcription start site, including the TATA box, to −281 relative to the E1A poly(A) site, including all of the major E1A splice sites (2, 31). Any transcripts detected from the *dl*312 template with primers near the 3′ end of E1A are likely to have a different stability than full-length E1A mRNAs transcribed from the wt and DM templates. This would make a comparison of the steady-state level of the E1A RNAs difficult to interpret in terms of the activity of the E1A promoter. Similarly, deletion of E1B control elements far upstream of the E1A poly(A) site within the E1A 3′ exon (32), as well as stimulation of E1B transcription by read-through transcription from E1A (33), also complicate interpretation of results for E1B.

We also analyzed the effects of alanine substitutions in the individual acidic regions N terminal and C terminal to CR3 [aa 133 to 138, as well as the (EP)6 repeat, aa 189 to 200] (Figures 2-4a – 2-4d). Deletions of each of these regions individually decreased luciferase activation ∼50% in the transient-transfection assay (Figure 2-3b, compare 133-205, 133-189, 140-205, and 140-189). However, in infected HBTECs expressing equal wt and mutant E1A protein at 12 h p.i., multialanine substitutions in the 6EP region just C terminal to CR3 (6EP-12A) had a much greater effect on E2, E3, and E4 transcription than mutation of the acidic region aa 133 to 138 (DDEDEE) just N terminal to CR3(133–138A) (Figures 2-4a – 2-4d).
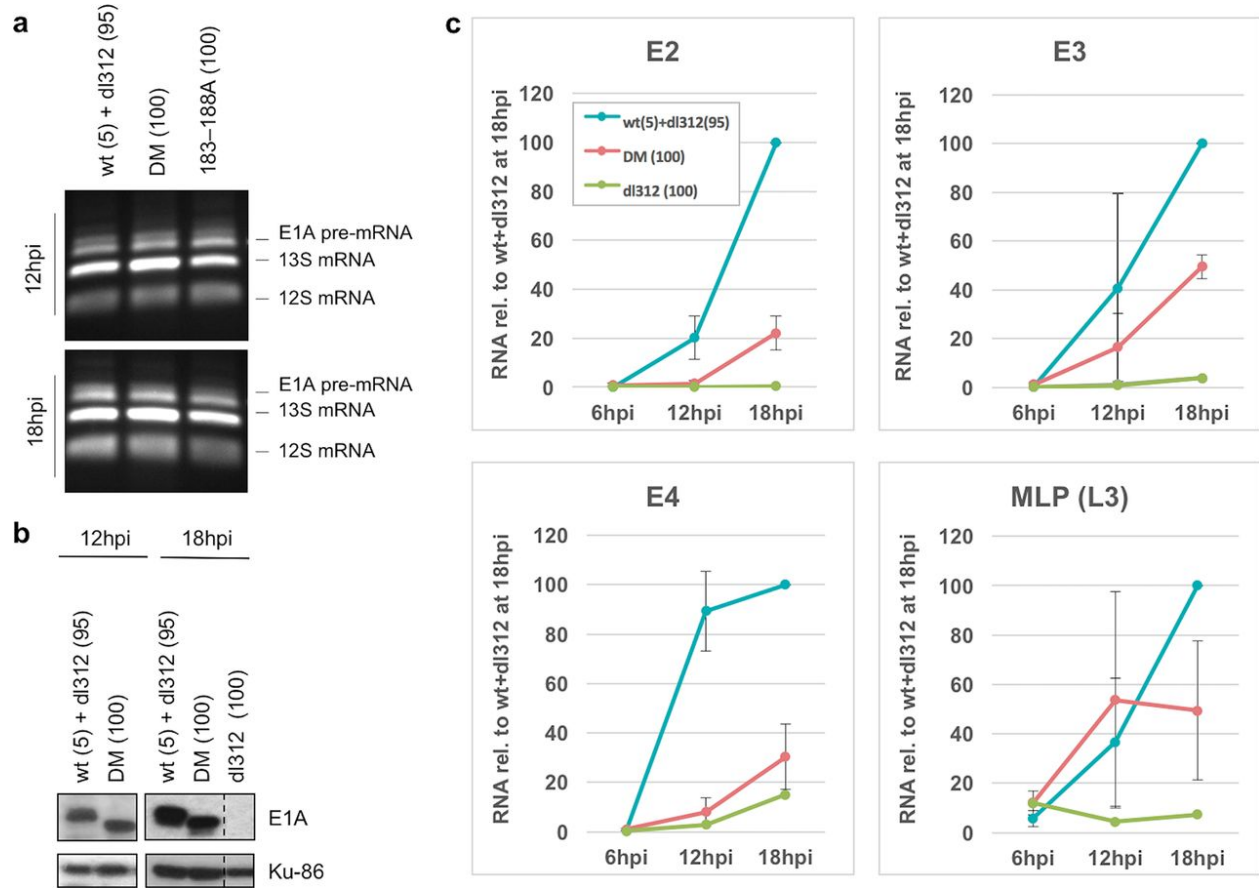
Figure 2-3: Activation of early viral promoters and MLP by wt and DM E1A.

(a) RT-PCR using primers spanning the major E1A splice sites with total cell RNA from HBTECs coinfected with the wt E1A-expressing virus at an MOI of 5 and *dl*312 at an MOI of 95 or infected with the DM or 183-188A vectors alone at an MOI of 100. The lengths of the pre-mRNA, 12S, and 13S transcripts are indicated. Only the region of the gel with visible bands is shown.

(b) Western blot showing wt and DM large E1A protein levels at 12 and 18 h p.i. HBTEC cells were coinfected with the wt E1A-expressing virus at an MOI of 5 and *dl*312 at an MOI of 95 or infected with the DM virus alone at an MOI of 100. Ku-86 protein levels were used as loading controls.

(c) Relative E2, E3, E4, and L3 RNA in infected HBTECs at the indicated times p.i., as assayed by qRT-PCR. HBTECs were infected with the *dl*312, wt and *dl*312, and DM viruses at the same MOIs as those described for panel a. Values are plotted relative to those of wt and *dl*312 at 18 h p.i. Data are represented as averages ± standard deviations (SD) from three independent experiments.
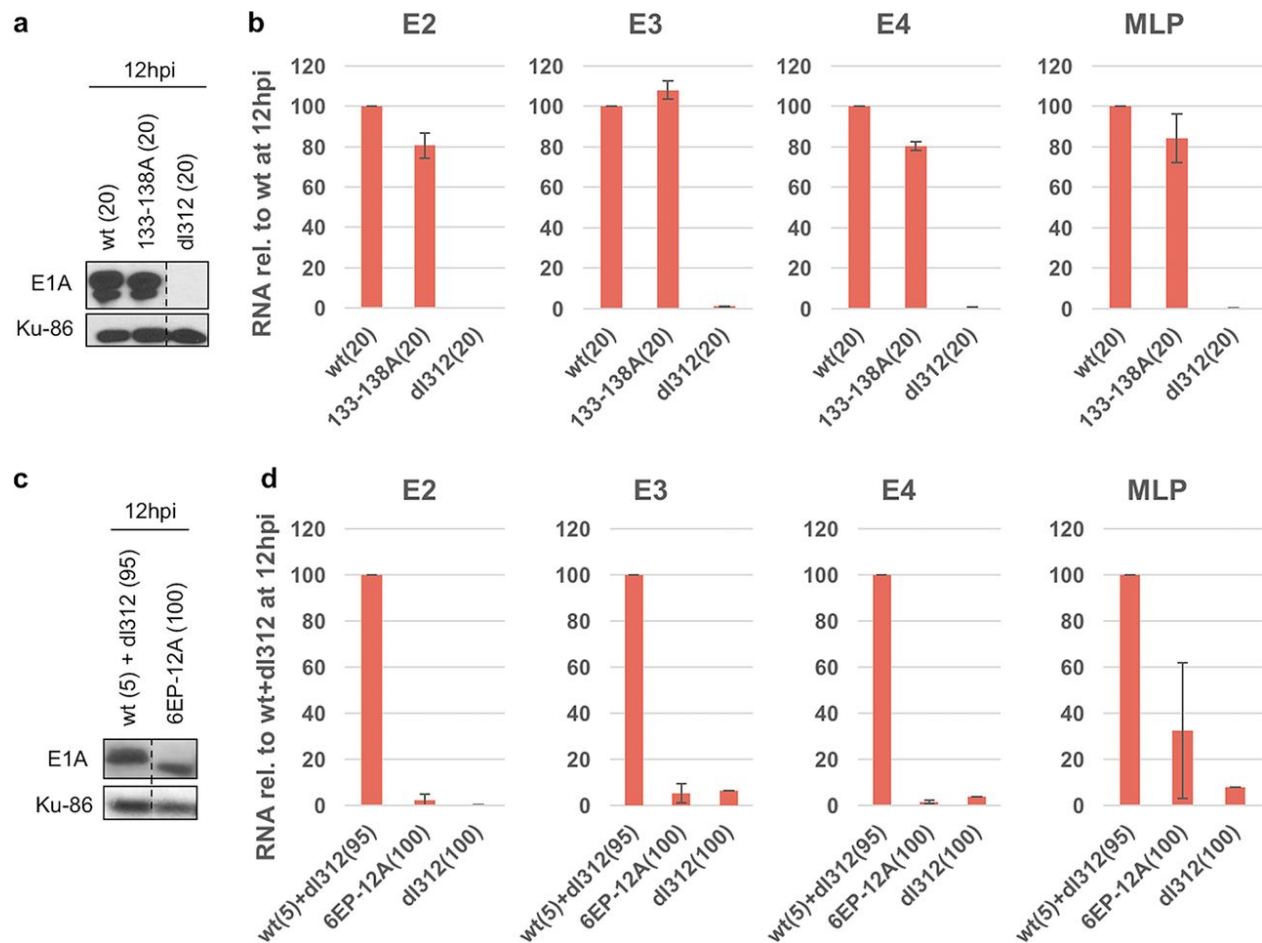
Figure 2-4: Activation of early viral promoters and MLP by wt and single acidic region mutant E1As

(a) Western blot showing wt and 133−138A mutant large E1A protein levels at 12 h p.i. HBTECs were infected with wt or 133−138A E1A-expressing virus at MOIs of 20. Ku-86 is a loading control.

(b) Relative E2, E3, E4, and L3 RNA levels in infected HBTECs at 12 h p.i., as assayed by qRT-PCR. Cells were infected with the wt and 133−138A E1A-expressing virus at the same MOIs as those described for panel a. Values are plotted relative to those of the wt at 12 h p.i. Data are represented as averages ± SD from three independent experiments.

(c and d) As described for panels a and b, except the 6EP-12A mutant was used. For experiments using this mutant, HBTECs were coinfected with the wt E1A-expressing virus at an MOI of 5 and *dl*312 at an MOI of 95 or infected with the 6EP-12A mutant E1A-expressing virus alone at an MOI of 100.

E1A amino acids 183 to 188 contribute to activation of early promoters E2, E3, E4, and MLP by binding multisubunit mediator complexes.

An additional Ad5 E1A mutant was constructed with alanine substitutions in the aa 183 to 188 region (VYSPVS), corresponding to a sequence found just C terminal to the Zn-finger region in large E1A proteins that is precisely conserved in all primate adenoviruses (4). This invariable E1A sequence is in the region required for binding multisubunit mediator complexes, as assayed by colocalization with both YFP-MED23 and YFP-MED6 at the *lacO* array in CHO-A03.1 cells (Figures 2-2c and 2-2c and Table 2-1). A serine residue in this region (aa 185) was left unsubstituted to avoid mutation of bases required for RNA splicing at the E1A 3′ splice site. In fact, the 183–188A E1A mutation had little effect on the ratio of unspliced E1A pre-mRNA to the spliced E1A mRNAs or the relative ratio of the 12S to 13S E1A mRNAs (Figure 2-3a). Early viral gene expression in infected HBTECs expressing equal wt and 183-188A mutant E1A protein levels was assayed by qRT-PCR at 18 h p.i. (Figure 2-5a). As expected, the E1A 183–188 region was required for most E1A activation of E2, E3, E4, and, to a lesser extent, the MLP (Figure 2-5b). This is consistent with the requirement of this region for binding multisubunit mediator complexes (Figure 2-2d and Table 2-1) and its crucial function in the transient-transfection assay (Figure 2-2b compare 133-189 to 133-178).

Taken together, these experiments indicate that the acidic region C terminal to CR3, the (EP)6 repeat, named AR1, for auxiliary region 1, by Ström et al. (18), contributes to E1A activation of early promoters E2, E3, and E4 during viral infection of human respiratory epithelial cells through an interaction with p300 and most likely the closely related host protein CBP. Further, E1A(aa 183–188) is essential for E1A activation of the early viral promoters E2,

E3, and E4 and additionally the low MLP activity early in infection, probably because they are

required for E1A to interact with multisubunit mediator complexes.
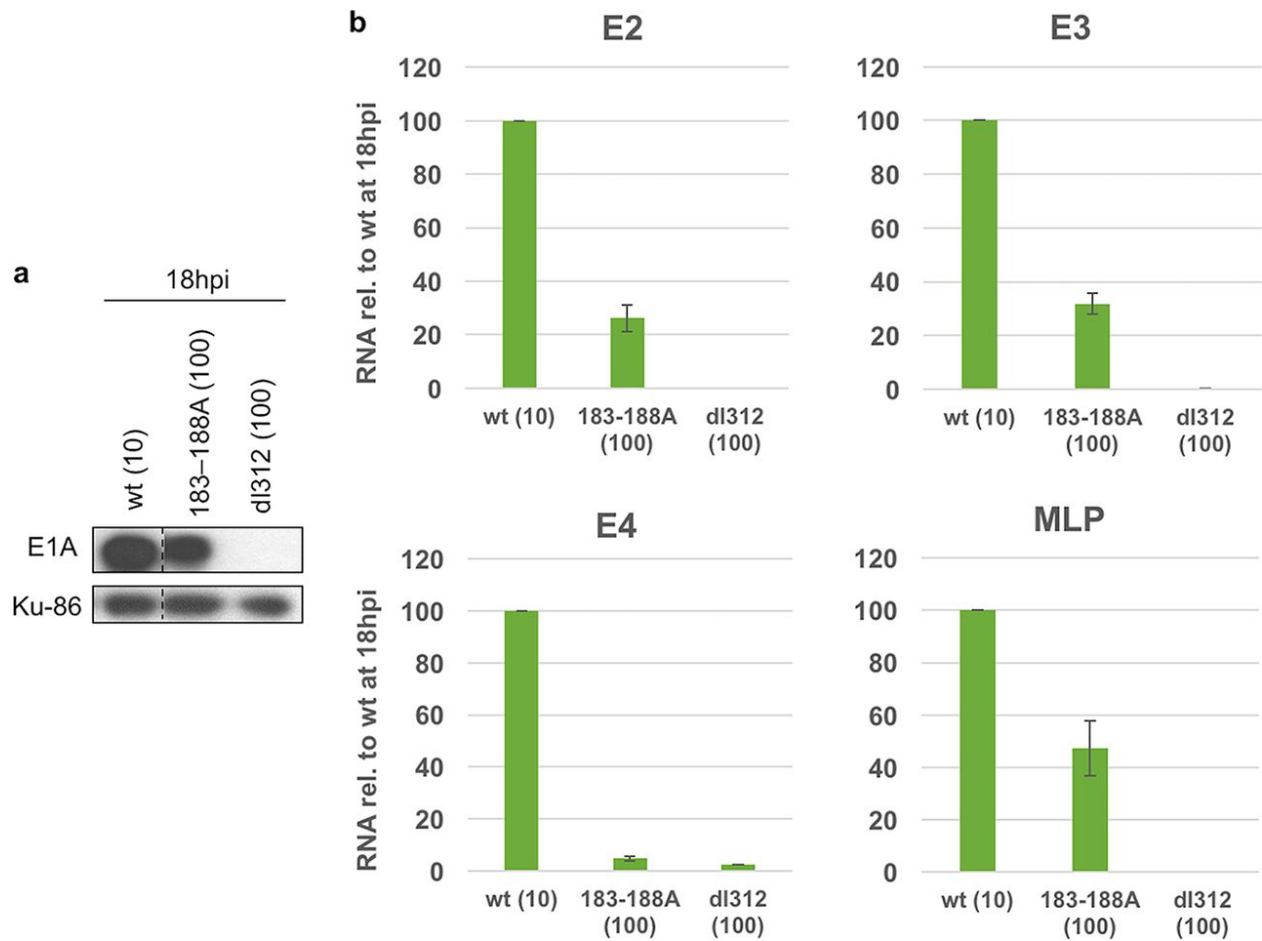
Figure 2-5: Activation of early viral promoters and MLP by wt and 183–188A mutant E1A.

(a) Western blot showing wt and 183–188A large E1A protein levels at 18 h p.i. HBTECs were infected with the wt E1A-expressing virus at an MOI of 10 or with the 183–188A mutant-expressing virus at an MOI of 100. Ku-86 protein is a loading control.

(b) Relative E2, E3, E4, and L3 RNA levels in infected HBTECs at 18 h p.i., as assayed by qRT-PCR. HBTECs were infected with the wt and 183–188A E1A-expressing virus at the same MOIs as those for panel a. Values are plotted relative to those of the wt at 18 h p.i. Data are represented as averages ± SD from three independent experiments.

Differences in E1A mutant-induced histone H3 acetylation at the early adenovirus promoters and their influence on RNA polymerase II preinitiation complex assembly and transcription.

Because p300/CBP is primarily responsible for mediating the acetylation of histone H3 at lysines 18 (H3K18) and 27 (H3K27) (6, 10, 34), we performed ChIP-seq for these modified histones and aligned reads to the Ad genome in HBTECs infected with virus expressing wt E1A at an MOI of 20 at 12 and 18 h p.i. Clear H3K18ac and H3K27ac peaks at the E1A, E2early, and E3 promoters and smaller peaks at the E4 promoter were observed, primarily downstream of the transcription start sites (TSSs) (0 to +1 kb) (Figure 2-6). These peaks coincided with GCN5/PCAF-mediated H3K9ac, which is also generally enriched around TSSs of active genes (35)(Figure 2-6). Peaks for H3K9ac were also observed at the E1B promoter, and smaller peaks for H3K18/27ac were observed within the gene body of E1B. The time course of H3K9ac at some genes was slower than that of H3K18/27ac. At E1A, E1B, E2early, and E3, H3K9ac increased from 12 to 18 h p.i., whereas H3K18/27ac was maximal at 12 h p.i. The E2early and E3 TSSs demonstrated a clear absence of acetylated H3, indicating nucleosome-depleted regions upstream of the highly transcribed E2early and E3 TSSs (36), where preinitiation complexes have assembled, displacing nucleosomes. A single, high peak of H3K18/27ac was observed between the E2early and E3 TSSs (Figure 2-6), probably representing a single acetylated nucleosome between them.

To assay Pol II preinitiation complex (PIC) assembly, we also did ChIP-seq for TBP and Pol II. The TBP subunit of TFIID is the first protein to interact with a TATA box promoter during PIC assembly, while Pol II is one of the last (37). We clearly detected peaks for TBP and Pol II at the active early promoters E1A, E1B, E2early, E3, and E4. At the MLP, TBP association was detectable at 12 h p.i., with a larger peak at 18 h p.i. A Pol II peak at the MLP

became visible at 18 h p.i. The ChIP-seq signal for TBP at the two adenovirus genes transcribed

by RNA polymerase III, VAI and VAII, was approximately five times higher than the signal for

TBP at the early promoters transcribed by RNA polymerase II (Figure 2-6, TBP track with

expanded y axis at the bottom in gray).

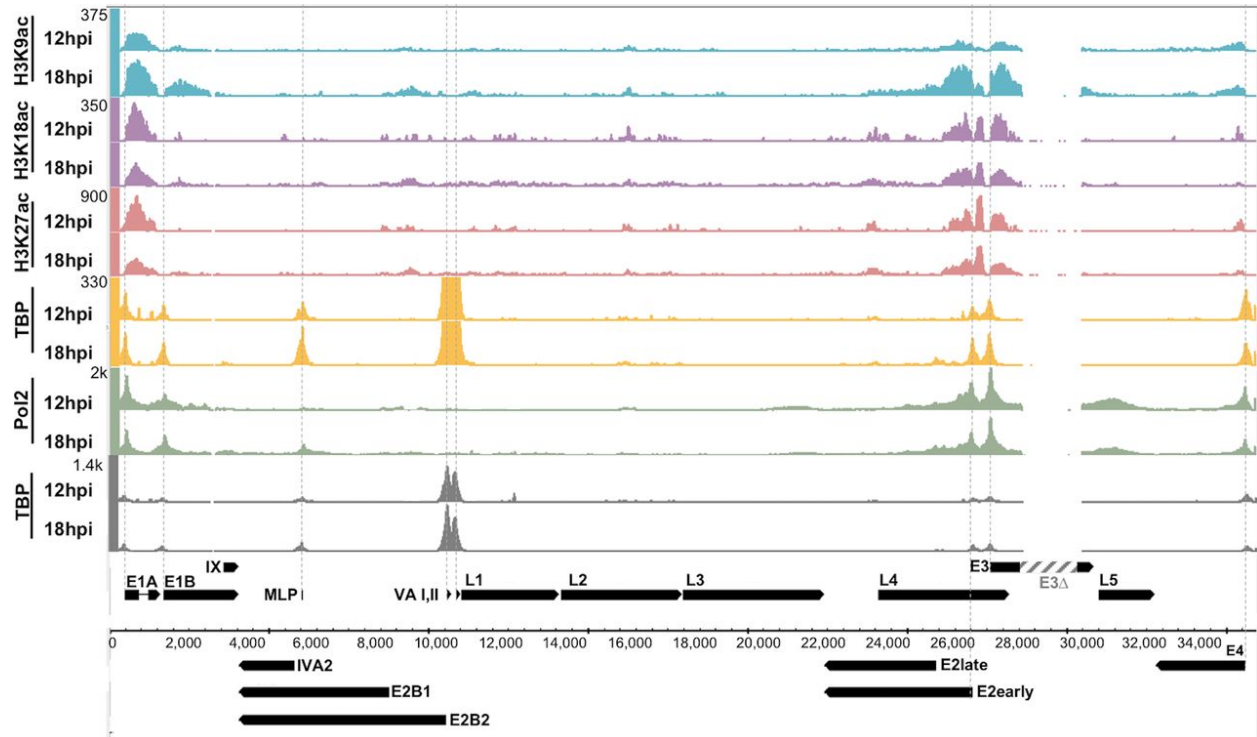***Figure 2-6: H3K9ac, H3K18ac, H3K27ac, TBP, and Pol II associated with the Ad5 genome.***
Genome browser plots of ChIP-seq normalized sequence tags in HBTECs infected with the wt
E1A-expressing virus at an MOI of 20. Dotted lines indicate TSSs for early regions (E1A, E1B,
E2early, E3, and E4), MLP, and VA I and II. ChIP-seq data for TBP are also shown at the
bottom plotted on an expanded *y* axis (gray).

To determine if the interaction of p300 with the E1A activation domain influences E2, E3, and E4 transcription via acetylation of histone H3 during infection, we also performed ChIP-seq for H3K18ac, H3K27ac, and H3K9ac in virus-infected HBTECs expressing equal concentrations of wt and DM E1A protein at 12 and 18 h p.i. We observed dramatic decreases in H3K18/27ac peaks at the E2early, E3, and E4 promoters in cells expressing DM E1A compared to wt E1A (Figure 2-7). ChIP-seq for H3K9ac revealed no decrease in H3K9 peaks at the E3 and E4 promoters and a decrease at the E2early promoter to about 50% of the control level.

Pol II and TBP ChIP-seq experiments were subsequently performed to determine if these differences in H3 acetylation were associated with differences in PIC assembly on the early viral promoters. Striking decreases in TBP and Pol II association induced by DM E1A compared to wt E1A correlated well with the observed decreases in H3K18/27ac at the E2early promoter. Apparently, the failure of the E1A DM to induce H3K18/27 acetylation at the E2early promoter completely blocked RNA polymerase II PIC assembly on the E2early promoter. In the same cells infected with the E1A DM and as discussed above in relation to the E2early promoter, H3K18/27ac also was virtually eliminated at the E3 promoter, with a TSS only 418 bp to the right of the E2early TSS. However, in contrast to the nearby E2early promoter, at the E3 promoter TBP association was only slightly reduced compared to that of cells expressing the same concentration of wt E1A, and there was no apparent decrease in RNA polymerase II association. These ChIP-seq data correlated well with the much greater effect of the E1A DM mutations on expression of E2early RNA compared to that of E3 RNA Figure 2-3c).

Surprisingly, and of considerable interest, TBP and Pol II association with the E4 promoter were only minimally decreased by the DM mutations (Figure 2-7), even though E4 RNA expression by the DM was nearly eliminated (Figure 2-3c). These results suggest that the

DM mutations block E4 transcription at a step subsequent to PIC assembly. Together these results demonstrate that the E2early promoter is regulated in part by p300/CBP-mediated acetylation of H3K18/27, which are required for a high level of Pol II PIC assembly, while H3K9ac appears to be sufficient for PIC assembly and moderate transcription at the E3 promoter. Interestingly, H3K18/27ac at the E4 promoter mediated by the p300 interaction with the E1A activation domain appeared to stimulate a step in transcription subsequent to TBP and Pol II association.
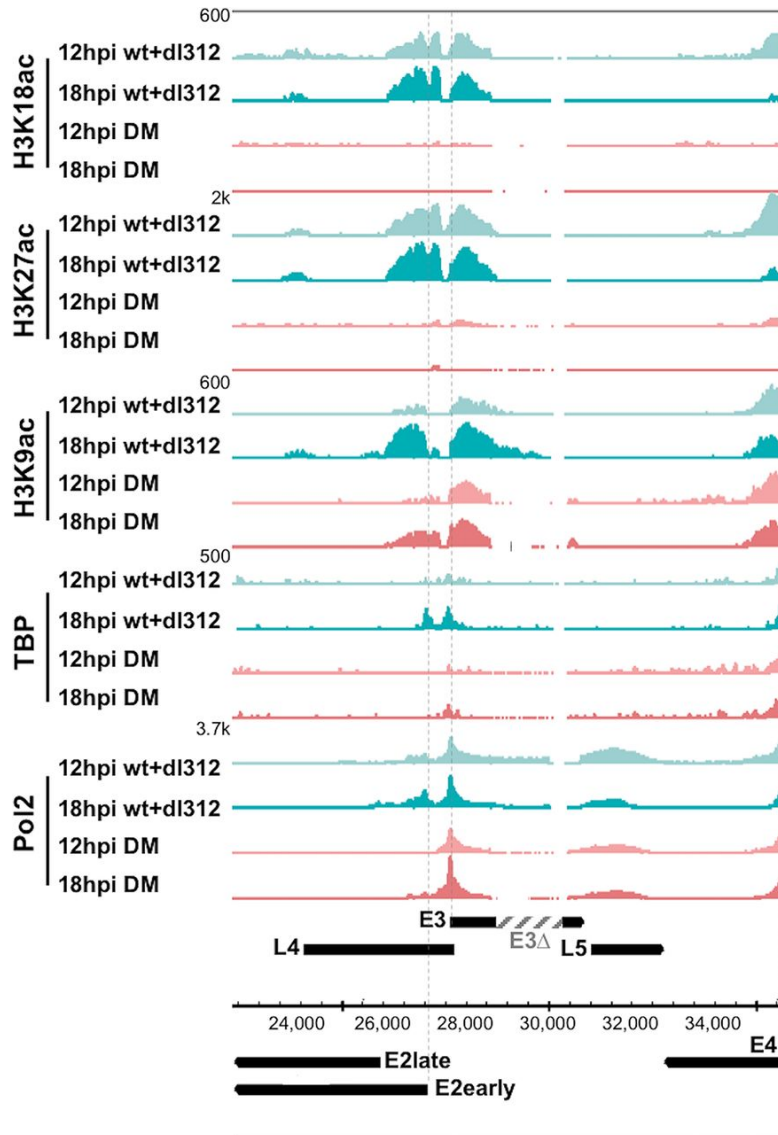
Figure 2-7: Defective H3 acetylation and PIC assembly by DM E1A at early viral promoters.
Genome browser plots of H3K9ac, H3K8ac, H3K27ac, TBP, and Pol II ChIP-seq normalized

sequence tags in HBTECs coinfected with the wt E1A-expressing virus at an MOI of 5 and *dl*312

at an MOI of 95 or infected with the DM vector alone at an MOI of 100. Dotted lines indicate

TSSs for early regions E2early, E3, and E4.

Discussion:

Although there is a well-established correlation between promoter and enhancer region histone N-terminal tail lysine acetylation and transcriptional activity (35), the mechanism(s) by which acetylation of histone lysines stimulates transcription is not well understood in most cases (38). The results presented here on regulation of adenovirus transcription by large E1A demonstrate that promoter region H3K18/27ac is required for different steps in gene activation at different adenovirus promoters.

Using colocalization of fluorescently labeled proteins in nuclei *in vivo*, we confirm an interaction between the strong E1A activation domain included in E1A(aa 133–205) and the acetyltransferase p300, as reported by Pelka et al. (1), on the basis of coimmunoprecipitation from transiently transfected cell extracts. We further mapped the partially redundant regions of E1A that bind p300 *in vivo* and show that this interaction with p300 contributes to H3K18/27ac, Pol II PIC assembly, and transcriptional activity of early viral promoters during viral infection of primary airway epithelial cells but to significantly different extents at each early promoter.

The regions of E1A required for the association of E1A(aa 121–223) with p300 were mapped to two acidic peptides flanking CR3, aa 133 to 138 (DDEDEE) and aa 189 to 200 (EPEPEPEPEPEP). This EP repeat was previously shown to contribute to maximal E1A activation of the early adenovirus promoters in transient-transfection assays with native E1A as opposed to Gal4DBD-E1A fusions and was named auxiliary region 1 (17, 18). The negative charge of the (EP)6 region is primarily responsible for its activity in this assay (18). Reducing the number of EP repeats reduced activation, a (DP)6 repeat and alanine substitutions of the prolines had activity similar to that of (EP)6, and an (AP)6 substitution was inactive (18). Deletion of both acidic regions resulted in the loss of p300 binding in our *in vivo* colocalization

assay and ~10-fold decreased activity in our transient-transfection reporter assays

using *lacI* fusions and a *lacO* reporter (Figure 2-2a) compare 140-189 to 121-223). Individually,

either of the two acidic regions was sufficient for p300 association in our *in vivo* colocalization

assay. However, the transient-transfection assay revealed that deletion of either region caused an

~2-fold decrease in activation function (Figures 2-2b and 2-2e). In contrast, infection of cells

with viruses containing multialanine substitutions in either or both of the two acidic regions

(133–138A and 6EP-12A mutants) showed that during infection, mutation of the 189–200 EP

repeat, equivalent to auxiliary region 1 (17, 18), was primarily responsible for the decrease in

transcriptional activation of E2, E3, and E4 by DM E1A (Figure 2-3). The greater effect of the

EP repeat on activation may also extend to E1A proteins from human adenoviruses other than

the respiratory adenoviruses in species C, since they contain a considerably longer peptide linker

between the N-terminal acidic region and the beginning of CR3 (39). It is also interesting that

these two acidic regions are also present in small e1a, although they are likely positioned

differently relative to each other in the absence of the intervening CR3. Despite the presence of

these two acidic regions in small e1a (Figure 2-2), in coimmunoprecipitation assays, small e1a

binds p300 only through the well-characterized interaction between the e1a N terminus and CR1

and the p300 equivalent of the CBP TAZ2 domain (1, 6, 8).

A revised model for functions of E1A activation subdomains.

Earlier, we found that the C4-Zn-finger region of large E1A(aa 140–178) (28)is required

for E1A binding to multisubunit mediator complexes required for *in vitro* transcriptional

activation by Gal4 fusions to E1A and other activation domains (21). The same E1A Zn-finger

region amino acids required for binding to multisubunit mediator complexes also were required

to bind free MED23 mediator subunits in excess over multisubunit mediator complexes in HeLa

nuclear extracts (21). These results, plus the observation that overexpression of MED23 inhibits,

or squelches, E1A activation and not activation by Gal4-VP16 led to the conclusion that E1A

binds multisubunit mediator complexes by binding the MED23 mediator subunit. This

conclusion was further supported by knockout of the mouse *Med23* gene, which generated cells

that supported activation by the VP16 activation domain but not the E1A activation domain (40).

Further, *Med23−/−* murine embryonic fibroblasts (MEFs) infected at low MOI with wt mouse

adenovirus I (MAVI) failed to express the MAV early mRNAs, similar to the phenotype

observed for E1A-minus MAVI in wt MEFs (41).

Here, we report that the C-terminal six amino acids of CR3 (aa 183 to 188) that are

invariable in all primate adenoviruses (5) are necessary, in addition to the MED23-binding Zn-

finger, for E1A binding to multisubunit mediator complexes, as opposed to monomeric MED23.

To assay association of E1A deletions with multisubunit mediator complexes *in vivo*, we

analyzed nuclear colocalization of LacI-CFP-E1A fragment fusions with YFP-MED6 at

the *lacO* array in CHO-A03.1 cells (Figure 2-1g – 2-1l). MED6 is located in the mediator head

domain, distant from MED23 in the tail domain (23). Consequently, association of an E1A

deletion with both YFP-MED6 and YFP-MED23 (Figure 2-2c and 2-2d and Table 2-1) and

implies that the retained region of E1A binds multisubunit mediator complexes, as shown for

E1A(aa 121–223) by direct biochemical analysis (21). The requirement for aa 183 to 188 for the

E1A interaction with multisubunit mediator complexes explains the requirement of this region of

CR3 for transcriptional activation without invoking a promoter targeting function for this region

(15). During viral infection, E1A(aa 183–188) is required for activation of early promoters E2,

E3, and E4 (Figure 2-5). Our results described above suggest that this is because this invariant region of E1A is required for E1A interaction with multisubunit mediator complexes.

Amino acid substitutions in the completely conserved C-terminal region of CR3 are defective for activation of the viral E3 promoter in a transient-transfection assay (19). They are also dominant negative over wt E1A for activation. In contrast, while mutants in the Zn-finger region are also defective for E3 activation, they are not transdominant (19). These observations supported the model that the Zn-finger region of CR3 binds a limiting factor required for activation of the early viral promoters, while the C-terminal ~10 amino acids of CR3 target the resulting complex to the early viral promoters (15, 19). However, our results provide an alternative explanation for the dominant-negative phenotype of the C-terminal CR3 mutants. We observed that the E1A Zn-finger region alone binds MED23 (Figure 2-2c and Table 2-1, fragment 140-178), and that the invariant region of E1A immediately C terminal to the Zn-finger is additionally required to bind multisubunit mediator complexes (Figure 2-2c and 2-2d and Table 2-1). Based on these results, we propose that mutants in the invariant region compete with wt E1A for binding MED23 in multisubunit mediator complexes, because they have an intact Zn-finger region that binds MED23 (Figure 2-2a, blue, 140-178). However, they are defective for interactions with other mediator subunits required for activation and are therefore dominant negative over wt E1A. In contrast, mutations in the Zn-finger subdomain are recessive (17) because they do not compete with wt E1A for binding multisubunit mediator complexes via their MED23 subunit.

The large E1A activation domain.

The original model that divided the CR3 region into an activation domain and a promoter-binding domain came from studies of Gal4 fusions to E1A fragments in transient-transfection assays (15, 16). Those studies reported, for the first time, that E1A(aa 121–223) has high activation domain activity when fused to the Gal4 DNA-binding domain. N-terminal deletions of E1A(aa 121–223) fused to the Gal4 DNA-binding domain from E1A(aa 121–140) retained activation domain activity in the transient-transfection assays, as did C-terminal deletions to aa 178. Consequently, the activation domain was presumed to map to the Zn-finger region between aa 140 and 178 (Figure 2-2a, blue). However, we found that a LacI fusion to E1A(aa 140–178) did not activate a *lacI* reporter in a transient-transfection assay (Figure 2-2b). Similar results were observed for a Gal4-DBD fusion to E1A(aa 140–178) versus a fusion to E1A(aa 121–223) and a reporter with five Gal4 binding sites upstream of the E1B promoter (A. J. Berk, unpublished results). This apparent discrepancy is explained by the two acidic regions flanking CR3, one from aa 133 to 138 and another from aa 189 to 200, that are functionally redundant in the transient-transfection assay (Figure 2-2b). As a consequence, the E1A N-terminal deletion to 140 retains the C-terminal acidic region from aa 189 to 200, while the C-terminal deletion to 189 retains the functionally compensating N-terminal acidic region from aa 133 to 138.

The earlier model of an N-terminal activation and a short C-terminal promoter binding domain in CR3 was further supported by experiments involving fusions of known functional domains of the yeast Gal4 activator and the HSVI VP16 immediate-early activator to inactive deletions of E1A (15, 16). These experiments showed that E1A(aa 121–223) activated the Ad5 E4 promoter, that mutations in the Zn-finger region of this part of E1A prevent activation of the

E4 promoter, and that these Zn-finger region mutations can be compensated for by fusion of the VP16 activation domain. These results suggested that the Zn-finger region alone functions as an activation domain whose function could be replaced by the VP16 activation domain (15, 16). However, our observation that LacI-E1A(140–178) does not activate transcription indicates that the E1A Zn-finger region alone does not function as an activation domain. Rather, E1A(aa 179–189) is additionally required for activation domain activity because it is required for E1A binding to multisubunit mediator complexes. The defect in binding to multisubunit mediator complexes of E1A mutants in the aa 140 to 178 region can be compensated for by fusion of the VP16-AD, since it also interacts with multisubunit mediator complexes (42, 43).

As a Gal4 fusion, E1A(aa 121–223) stimulates the assembly of a PIC on a template with Gal4-binding sites (25). Presently, however, the mechanism by which the mediator interaction with native E1A (i.e., not fused to a DNA-binding domain) stimulates transcription remains unclear. We propose that wt E1A and an associated multisubunit mediator complex are targeted to early adenovirus promoters through interactions between activation domains of the cellular activators bound to early viral promoters and multisubunit mediator complexes. The interactions of TFIID and the Pol II general transcription factors with both viral promoters and the mediator probably also contribute to association of mediator complexes with associated E1A to early viral promoters. The low level of transcription from the early viral promoters in the absence of E1A is greatly stimulated by the high-affinity interaction of the E1A Zn-finger region with MED23 as well as additional interactions of E1A(aa 183–188) that result in binding to multisubunit mediator complexes. One possibility is that these E1A-mediator interactions induce a conformational change in the mediator that favors its association with Pol II, as has been proposed for other activation domains (23, 44, 45)

The E1A interactions with p300 do not greatly stimulate early transcription from the MLP.

At 18 h p.i., L3 is expressed at very low levels compared to the late phase of infection, when virus-encoded transcriptional activators bind in the first intron to stimulate transcription from the MLP several hundredfold (46). However, we observed ~20-fold activation by wt E1A of the low level of L3 RNA expression at 18 h p.i., presumably from the MLP. This can be seen by comparing L3 RNA in cells infected with a mixture of the wt E1A-expressing virus and *dl*312 virus and cells infected with *dl*312 alone (Figure 2-3c, MLP). However, this activation was not greatly dependent on the interaction of the E1A AD with p300, because it was not decreased by the E1A DM mutations at 12 h p.i. and was reduced only ~50% at 18 h p.i. (Figure 2-3c). Consistent with this, H3 acetylation was not observed at the MLP at 12 and 18 h p.i. with Ad expressing wt E1A (Figure 2-6).

TBP association at Pol II and Pol III promoters on the adenoviral genome.

It is remarkable that the ChIP-seq signal for TBP at the two adenovirus genes transcribed by RNA polymerase III, VAI and VAII, was approximately five times higher than the signal for TBP at the early promoters transcribed by RNA polymerase II (Figure 2-6, bottom, gray). This indicates that at the time of cross-linking, more viral DNA molecules are bound by the RNA polymerase III TBP-containing initiation factor TFIIIB than are bound by TFIID at the promoters of viral genes transcribed by Pol II. However, another likely possibility is that TBP is much more readily indirectly cross-linked to promoter DNA as a subunit of TFIIIB than as a subunit of TFIID. The complexes of TFIIIB with tRNA and 5S rRNA promoter DNA are stable to high salt and high concentrations of heparin (47). In contrast, RNA polymerase II preinitiation

complexes are disrupted by 0.5 M KCl (48). This implies that much more of the TFIIIB protein, comprised of TBP, BRF, and BDP subunits, contacts DNA in the Pol III preinitiation complex than does TFIID and other Pol II general transcription factors in a Pol II PIC. Further, in the crystal structure of a TBP-BRF-DNA complex (49), BRF interacts extensively with the convex top of TBP, and BRF helix 25 (absent in TFIID) extends along the downstream promoter DNA for six base pairs. This may increase the opportunity for cross-linking TBP to DNA indirectly through cross-links to BRF that is cross-linked to DNA.

Histone H3 acetylation at viral early promoters

Histone lysines H3K18 and H3K27 are acetylated primarily by p300 and its closely related paralog, CBP (9, 10). We analyzed acetylation at these sites on histones associated with the viral genome early during infection by performing ChIP-seq in HBTECs infected with Ad5 mutants expressing wt E1A proteins and mapping the immunoprecipitated DNA sequences to the viral genome (Figure 2-6). We observed significant peaks of H3K18/27ac at the E1A, E2early, E3, and E4 promoters at 12 and/or 18 h p.i. but not at the E1B or MLP promoters (Figure 2-6). H3K18/27ac at the E2early, E3, and E4 promoters was greatly decreased following infection with the E1A DM defective for the E1A activation domain-p300 interaction. These results indicate that H3K18/27 acetylation at these promoters requires targeting p300/CBP to the promoters through their interaction with the acidic regions flanking CR3 [E1A(aa 133–138) and (EP)6 repeat, aa 189 to 200]. The virtual absence of H3K18/27ac at the E2early promoter following infection with the DM correlated with an absence of TBP and Pol II association, suggesting that H3K18/27ac by p300/CBP is required for E1A stimulation of Pol II preinitiation complex assembly *in vivo* at this promoter (Figure 2-7). Residual H3K9ac at the E2early promoter in cells expressing DM E1A was not sufficient for high levels of Pol II PIC assembly.

These observations are consistent with the model that hypoacetylated nucleosomes inhibit the

association of TFIID and other Pol II general transcription factors with promoter DNA, and that

histone acetylation makes the promoter elements more accessible to the GTFs. Histone tail

acetylation at these early viral promoters also may generate binding sites for proteins that

stimulate transcription, including proteins with bromodomains that bind acetylated lysines (50).

In contrast to the E2early promoter, H3K18/27ac is not required for significant levels of

PIC assembly or transcription from the nearby E3 promoter. (The E2early and E3 TSSs are

separated by only 418 bp.) H3K9ac in the absence of H3K18/27ac may be sufficient for PIC

assembly at the E3 promoter.

While hypoacetylated H3K18/27ac was observed at the E4 promoter in cells expressing

DM E1A, high levels of H3K9ac as well as TBP and Pol II association were observed. This

suggests that H3K18/27ac is not required for PIC assembly at the E4 promoter. However,

H3K9ac at the E4 promoter, which continues to occur in cells expressing the E1A DM, may be

sufficient for Pol II PIC assembly. Surprisingly, in cells infected with the E1A DM, we noted a

clear discrepancy between the TBP and Pol II ChIP-seq signals at the E4 promoter and the qRT-

PCR data for E4 mRNA. Pol II and TBP peaks were not reduced at the E4 promoter in DM-

infected cells (Figure 2-7), yet H3K18/27ac and E4 mRNA expression by the DM were greatly

decreased (Figure 2-3c) These results lead us to speculate that H3K18/27ac mediated by the

E1A-p300/CBP interaction at the E4 promoter regulates elongation of the polymerase, rather

than Pol II PIC assembly, as occurs at the E2early promoter. This model of E1A stimulation of

Pol II elongation from the E4 promoter may explain why H3 acetylation occurs primarily

downstream from the TSS (Figure 2-6). E1A has been previously shown to promote

transcriptional elongation at early viral genes by recruiting the hPaf1 complex (51). Perhaps

promoter region H3K18/27ac is required for E1A to stimulate hPaf1-dependent elongation at the E4 promoter.

H3K9ac peaks were present at the E2early, E3, and E4 promoters in addition to H3K18/27ac and were decreased after infection with the DM at the E2early promoter (Figure 2-7) This indicates that p300 recruitment by E1A and/or H3K18/27 acetylation regulate H3K9 acetylation at the E2early promoter. This decrease in H3K9ac may be because H3K9 is less accessible to acetyl transferases in the absence of H3K18/27ac or because PCAF/hGCN5, the acetyl transferases primarily responsible for H3K9 acetylation (10), are normally recruited to the E2early promoter through interactions with H3K18/27ac.

These patterns of H3 acetylation at early viral promoters in response to multialanine substitutions of subdomains of the E1A activation domain indicate that H3K18/27ac by p300/CBP is required for maximal H3K9 acetylation and the assembly of Pol II PICs at the E2early promoter. In contrast, Pol II PIC assembly on the E3 and E4 promoters is associated with H3K9ac but not H3K18/27ac. In the case of E3, this is sufficient for PIC assembly and moderate transcription. At the E4 promoter, the E1A activation domain-p300/CBP interaction is not required for TBP and Pol II association but is required for H3K18/27ac and transcription. This may be because elongation of paused Pol II at the E4 promoter is dependent on H3K18/27ac. By eliminating the association of the E1A activation domain with p300, we have revealed striking diversity in transcriptional regulation of the viral genome early in infection, including nuanced roles for p300/CBP at each early viral promoter.

Chapter 3: ADENOVIRUS EARLY PROMOTER E4 IS REGULATED DURING TRANSCRIPTIONAL ELONGATION BY H3K18/27AC DEPENDENT SEC RECRUITMENT

Introduction

In addition to PIC assembly and initiation, the transition from promoter-proximal paused to productively elongating Pol2 serves as a key step in transcriptional regulation. After the recruitment of Pol2 by the GTFs and the formation of the PIC, transcription initiation occurs concurrently with the phosphorylation of Ser5 on the Pol2 heptapeptide repeat C-terminal domain (CTD). Pol2 then transcribes approximately 30-60 bases downstream of the transcription start site (TSS) and pauses, where it is stabilized by negative elongation factor (NELF) and DRB-sensitivity inducing factor (DSIF) (52, 53). Recruitment of the super elongation complex (SEC) including P-TEFb and its enzymatic subunit CDK9 results in the phosphorylation of NELF, DSIF, and Ser2 on the Pol2 CTD, whereupon NELF dissociates and Pol2 is released and proceeds to productive elongation (52, 53).

Histone acetylation is well known to contribute to a permissive chromatin state for Pol2 PIC assembly at active promoters, and there is recently published work concerning its role in facilitating transcriptional elongation as well. For example, the chromatin reader protein BRD4 is thought to recruit pTEF-b to transcription start sites and serves as a Pol2 elongation factor dependent on its interactions with acetylated histones through its bromodomains (54). In addition, H3 acetylation mediated by the Drosophila CBP homolog stimulates productive elongation past the +1 nucleosome (55). Recruitment of the yeast histone chaperone FACT by acetylated H3 has also been shown to stimulate elongation (56).

The SEC is a multi-subunit complex comprised of P-TEFb along with AF4/FMR2 (AFF) proteins AFF1/4, ELL protein family members ELL1/2/3, ELL-associated factors EAF1/2, and the highly homologous YEATS domain-containing proteins AF9 or ENL. There are various forms of the SEC including SEC-like complexes, which contain different combinations of

elongation factors suggesting diversity in their regulatory mechanisms (57). P-TEFb, a central

AFF scaffold protein, and ENL or AF9 are consistent components of SEC complexes. AF9 and

ENL been functionally linked to SEC recruitment to chromatin and positive regulation of

elongation through interactions with the PAF1c complex (58) and DOT1L which deposits the

active chromatin modification H3K79me (59). Importantly, AF9 and ENL YEATS domains

have been demonstrated to recognize active chromatin marks H3K9ac and H4K15ac (60), and to

a lesser extent, H3K18/27ac (59), and are essential for SEC-dependent activation of a luciferase

reporter driven by the HIV-1 LTR (58). Despite these conclusions, the functional role of histone

acetylation during this critical regulatory step remains poorly understood.

We have previously identified regulation of the early adenovirus promoter E2early by

H3K18/27ac via an interaction between p300 and the E1A AD at the stage of transcriptional

initiation (61). However, at the E4 promoter, PIC assembly was not affected by loss of p300

binding by E1A, despite significantly decreased H3K18/27ac and E4 RNA by the p300-binding

mutant E1A protein (termed the "double mutant", or DM). This result was particularly striking as

it suggested that the E4 promoter is regulated by H3 acetylation at a step in transcription

subsequent to TBP and Pol2 association, possibly during release of promoter-proximal paused

Pol2.

In order to investigate the role of H3K18/27ac on transcriptional elongation at E4, we

mapped the association of transcriptionally active Pol2 on the Ad5 genome using GRO-seq

(Global Run-On sequencing) (62). We found defective paused Pol2 release at E4 in cells

expressing DM E1A, consistent with the previously shown decreases in H3K18/27ac and E4

RNA. ChIP-seq for SEC components CDK9, BRD4, AF9, and ENL demonstrated decreased

SEC recruitment to E4 by DM E1A. Using the specific p300 HAT inhibitor A485, we

determined that p300 HAT activity was essential for efficient paused Pol2 release and SEC recruitment at E4. We also extended our studies to the human genome, where we found that A485 treatment causes defective pause release at a subset of genes, where H3K18ac is greatly decreased at TSSs. These differences correlate with decreased SEC component binding at these genes, similar to what we observed at E4. Together, our results propose a mechanism of SEC recruitment by H3 acetylation during the transition to productively elongating Pol2.

Results

H3K18/27ac by p300 stimulates paused Pol2 release at E4

Previous work from our lab has shown that transcriptional regulation of E4 by H3K18/27ac resulting from recruitment of CBP/p300 by the E1A activation domain occurs subsequent to PIC assembly (15). To analyze the effect of H3K18/27ac on Pol2 elongation through E4, we applied the GRO-seq method (1).To avoid possible effects of cellular mutations in stable cell lines, we performed these studies in primary human bronchial-tracheal epithelial cells (HBTECs). HBTECs were infected with Ad5 mutant vectors expressing wt E1A or a mutant E1A designated "DM" containing poly-alanine substitutions in two previously identified, highly acidic regions of E1A flanking CR3 that interact with p300 in vivo (15). Multiplicities of infections were carefully adjusted to yield equal steady-state amounts of wt E1A and the less stable DM (15). Infections were performed with an moi of 100 for the DM, or an moi of 5 the for the mutant expressing wt E1A plus an moi of 95 with the E1A deletion mutant *dl312* to maintain equal copies of viral DNA with the early transcription units in cells expressing equal amounts of the wt and DM E1A proteins. GRO-seq data at 12 hours post infection (hpi) revealed peaks of paused Pol2 at the expected location 40-60 bp downstream from the E3 and E4 TSSs (Figure 3-

44

1a). To determine the degree of pausing, we calculated the pausing index (PI, (1)), or the number

of reads in the promoter-proximal region (TSS to +200bp) relative to the reads in the gene body

(+201 to TTS) in cells expressing wt E1A. We compared the PIs in cells expressing wt and DM

E1A. With the DM, the PI at E4 increased almost 2-fold (wt PI=1.37 vs. DM PI= 2.33) while

there was less of a decrease at E3 (wt PI=1.41 vs. DM PI=1.65) (Figure 3-1b). For E3, we

divided the counts in the promotor proximal region by a region of the gene body that extended

from +201 to the beginning of the E3 deletion, to avoid discrepancies in gene body lengths due

to different deletions in the dl312 and DM mutant vectors (diagrammed in the browser track

annotations in Figure 3-1a). Therefore, loss of H3K18/27ac at E4 causes a defect in proximal

paused Pol2 release, with less of an effect at E3. This result compliments our previous data

which showed regulation of E3 is minimally effected by H3K18/27ac (15).

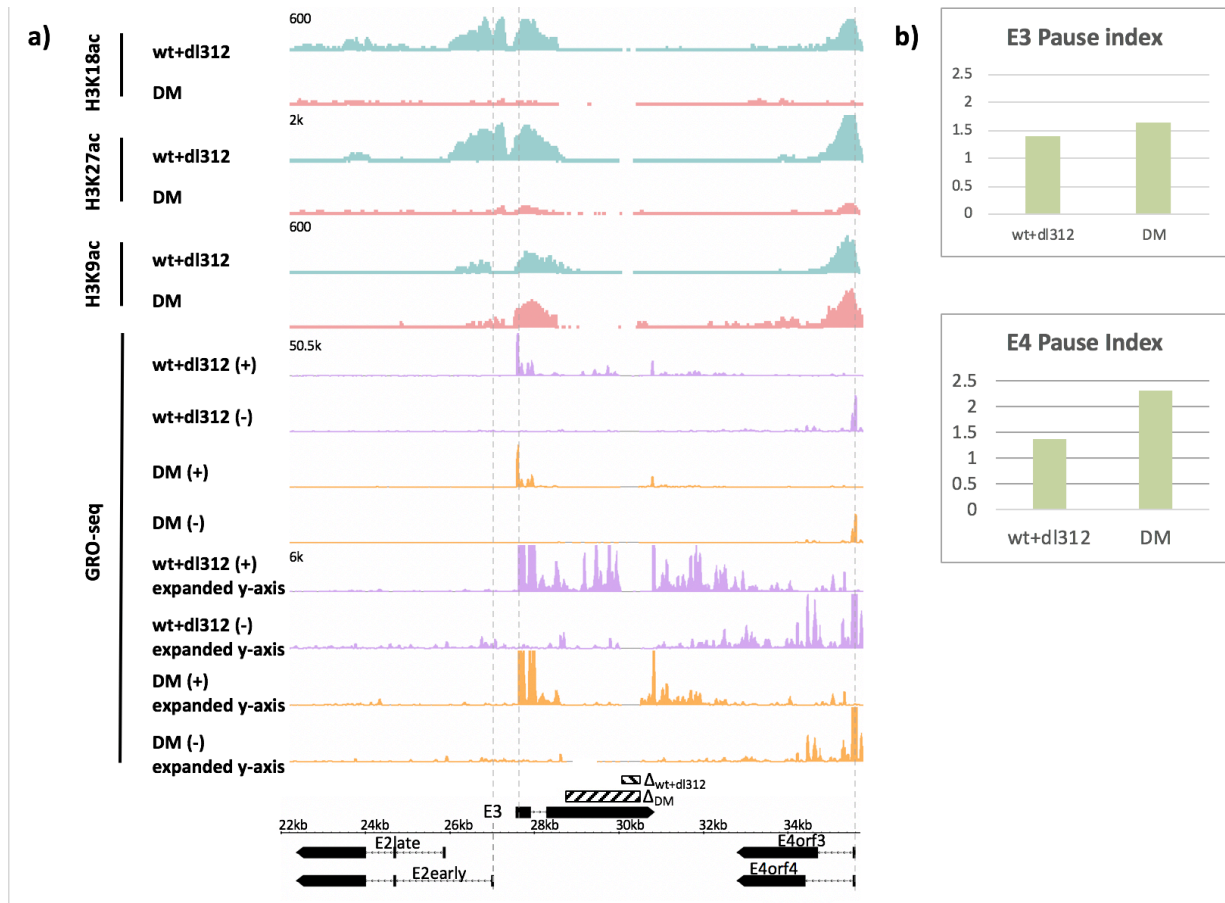***Figure 3-1: H3K18/27ac by p300-E1A AD stimulates paused Pol2 release at E4***

(a) GRO-seq in cells infected with wt+dl312 or DM, plotted with H3K18ac, H3K27ac and

H3K9ac ChIP-seq (61) on the Ad5 genome. GRO-seq tracks are shown with two different y-axis.

(b) Pause indexes for E3 and E4 in cells expressing wt E1A or DM. Pause index is defined as the

ratio of: reads in the promoter region to reads in the gene body.

Defective Pol2 pausing at E4 correlates with decreased binding of SEC subunits CDK9, AF9, and ENL

Phosphorylation of Ser5 on the Pol2 CTD by the CDK7 subunit of TFIIH occurs during transcriptional initiation, and Ser2, NELF, and DSIF phosphorylation by the CDK9 subunit of P-TEFb allows for paused Pol2 release and the transition to productive elongation. In order to characterize these mechanisms on the Ad5 genome, we performed ChIP-seq for Ser5-P, Ser2-P, NELF, and CDK9 in cells expressing wt E1A. At E2early, Ser 5-P peaked at the TSS and decreased throughout the gene body. We observed two Ser2-P peaks in the E2early gene body-one just downstream of the TSS, likely indicating paused Pol2, and another peak just upstream of the E2early second exon. A small Ser5-P peak is also observed at this position (Figure 3-2a). This can be explained by the known reduction in elongation rate at spliced exons which mediates splice site recognition and spliceosome assembly (63, 64). Both CDK9 and NELF peaks occurred at the expected E2early pause site (Figure 3-2a). At E3, Ser5-P also peaked at the TSS and decreased throughout the gene body, and Ser2 onset began at the TSS and increased throughout the gene body. CDK9 and NELF peaks also occurred at the expected E3 pause site (Figure 3-2a). At E4, Ser5-P peaked at the TSS and decreased through the gene body, similar to what was observed at E2early and E3. Ser2-P peaked just downstream of the TSS, likely indicating paused Pol2, decreased elongation rate prior to the 3' splice site in the E4orf3 transcript, or both. CDK9 and NELF peaks at E4 again occurred at the expected pause site.

We next asked if defective paused Pol2 release by DM E1A is due to decreased recruitment of P-TEFb containing complexes. A large percentage of P-TEFb exists in complex with the 7SK snRNP, where CDK9 activity is inhibited and it is sequestered from chromatin (65–67). Eviction of PTEF-b from 7SK snRNP enables its integration into complexes with

activated CDK9 kinase activity, including a complex with BRD4 (BRD4-PTEFb) and the super

elongation complex (SEC) (68). Integration into both these complexes allows CDK9 to be

targeted to promoters and enhancers where it phosphorylates its targets and stimulates paused

Pol2 release (54). In order to determine the effects of H3K18/27ac on active P-TEFb complex

recruitment, we performed ChIP-seq for CDK9, and AF9, ENL, and BRD4 on the Ad5 genome.

In response to H3K18/27 hypoacetylation by DM E1A, there is significantly decreased CDK9,

AF9, and ENL binding at the E2early, E3, and E4 promoters and gene bodies (Figure 3-2b).

Importantly, we did not see decreases in AF9 and ENL at the TSSs of human genes,

demonstrating the specificity of this effect at these viral genes (Figure 3-2c). BRD4 association

at TSSs did not change at E4 and was only moderately decreased at E3, with the only marked

decrease occurring at the E2 TSS. These data demonstrate that H3K18/27ac facilitates paused

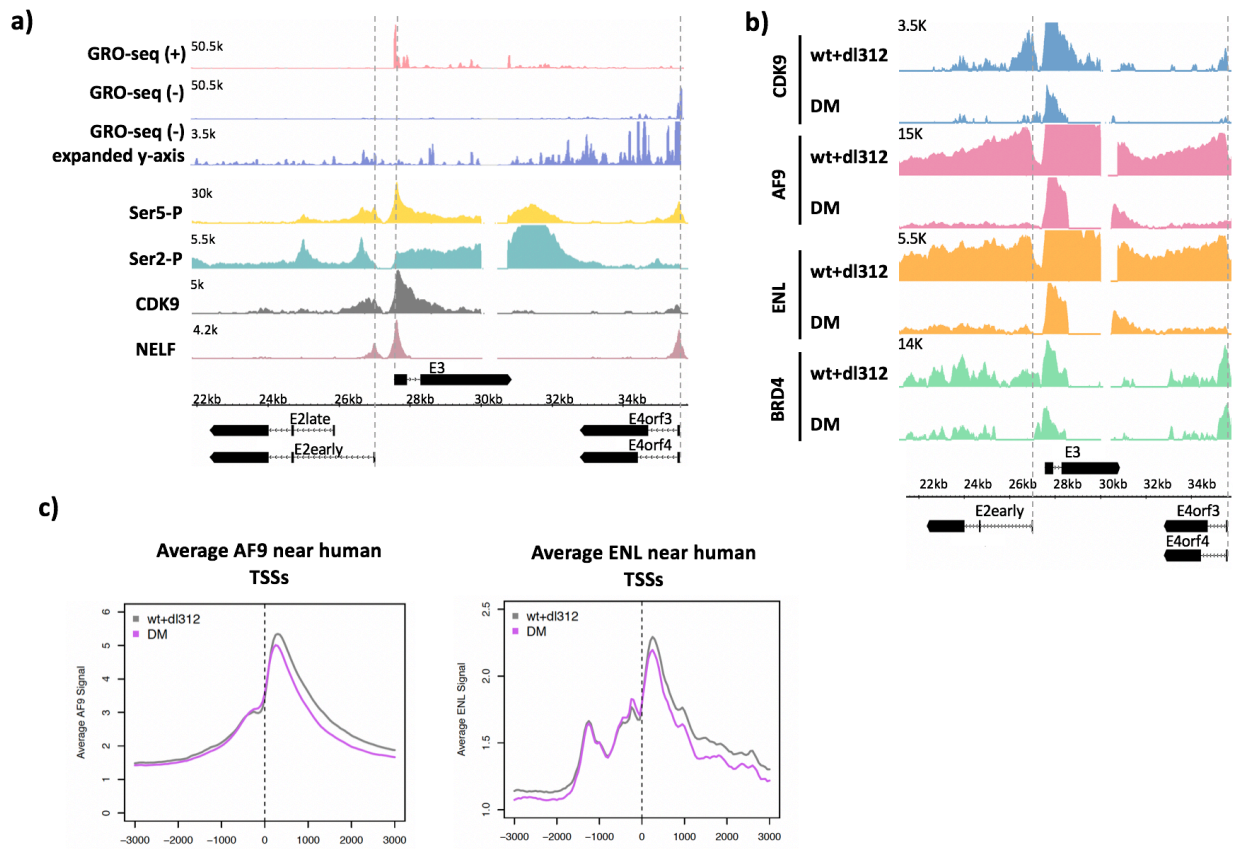Pol2 release at E4 mainly through the recruitment of the SEC.

Figure 3-2: Ser5-P, Ser2-P, CDK9, NELF, and SEC subunit association on the Ad5 genome

(a) Ser5-P, Ser2-P, CDK9, and NELF ChIP-seq plotted with GRO-seq in cells expressing wt
E1A.

(b) CDK9, AF9, ENL, and BRD4 ChIP-seq in cells expressing wt or DM E1A.

(c) Average plots of AF9 and ENL binding near TSSs on the human genome.

P300 histone acetyl-transferase activity is required for Pol2 pause release and recruitment of
AF9, ENL, and BRD4 at E4

A485 is a potent and specific small molecule inhibitor of p300/CBP's acetyl transferase

activity (69). Decreased H3K18ac after A485 treatment in HBTECs was confirmed by western

blot (Figure 3-3a). H3K9/18/27ac ChIP-seq on the Ad5 genome in wt E1A infected cells treated

with A485 demonstrated greatly inhibited H3K18/27ac, and some inhibition of H3K9ac at early

viral promoters (Figure 3-3a). In order to distinguish the effects of p300 HAT activity vs.

possible recruitment of other co-activator proteins by p300 on the transcription of early viral

genes, we assayed pre-mRNA levels using qRT-PCR with RNA isolated from HBTECs

expressing wt E1A treated with A485 or DMSO. We saw decreases in E2early and E4 pre-

mRNA, while E3 pre-mRNA was decreased only moderately with A485 treatment (Figure 3-3b).

Decreases in early RNAs with A485 treatment were not as dramatic as what we observed with

loss of p300 binding by DM E1A (61). This was expected, considering A485 does not decrease

H3K18/27ac to the same extent. However, in both cases, we saw the greatest decreases at E4 and

E2early.

We next asked if p300 HAT activity is required for release of paused Pol2 at E4. To

answer this question, we performed GRO-seq in wt E1A infected HBTECs treated with DMSO

or A485 and calculated the corresponding pausing indexes (Figure 3-4a,b). There was no

difference in PI at E2early (DMSO PI=0.13, A485 PI=0.12) or E3 (DMSO PI=1.2, A485

PI=1.89), and an increase in PI at E4 with A485 treatment (DMSO PI=0.79, A485 PI=1.13)

(Figure 3-4b). These results are consistent with our GRO-seq data with DM E1A infection, and

demonstrate that p300 HAT activity, and not solely the possible recruitment of other co-

activators by p300, is necessary for paused Pol2 release at E4.

To see if inhibition of p300 HAT activity resulted in defective SEC recruitment at E4, we performed AF9, ENL, and BRD4 ChIP-seq in wt E1A infected cells after DMSO or A485 treatment. Similar to cells expressing DM E1A, we saw decreases in AF9 and ENL association at E2early, E3, and E4 in cells treated with A485. We also saw decreases in BRD4 at these promoters, which may be explained by the slight decrease in H3K9ac observed after treatment with A485 (Figure 3-3a). These data suggest a model where E4 is regulated during transcriptional elongation by SEC and BRD4 recruitment, dependent on H3 acetylation mediated by the interaction between p300 and E1A AD (Figure 3-4d).
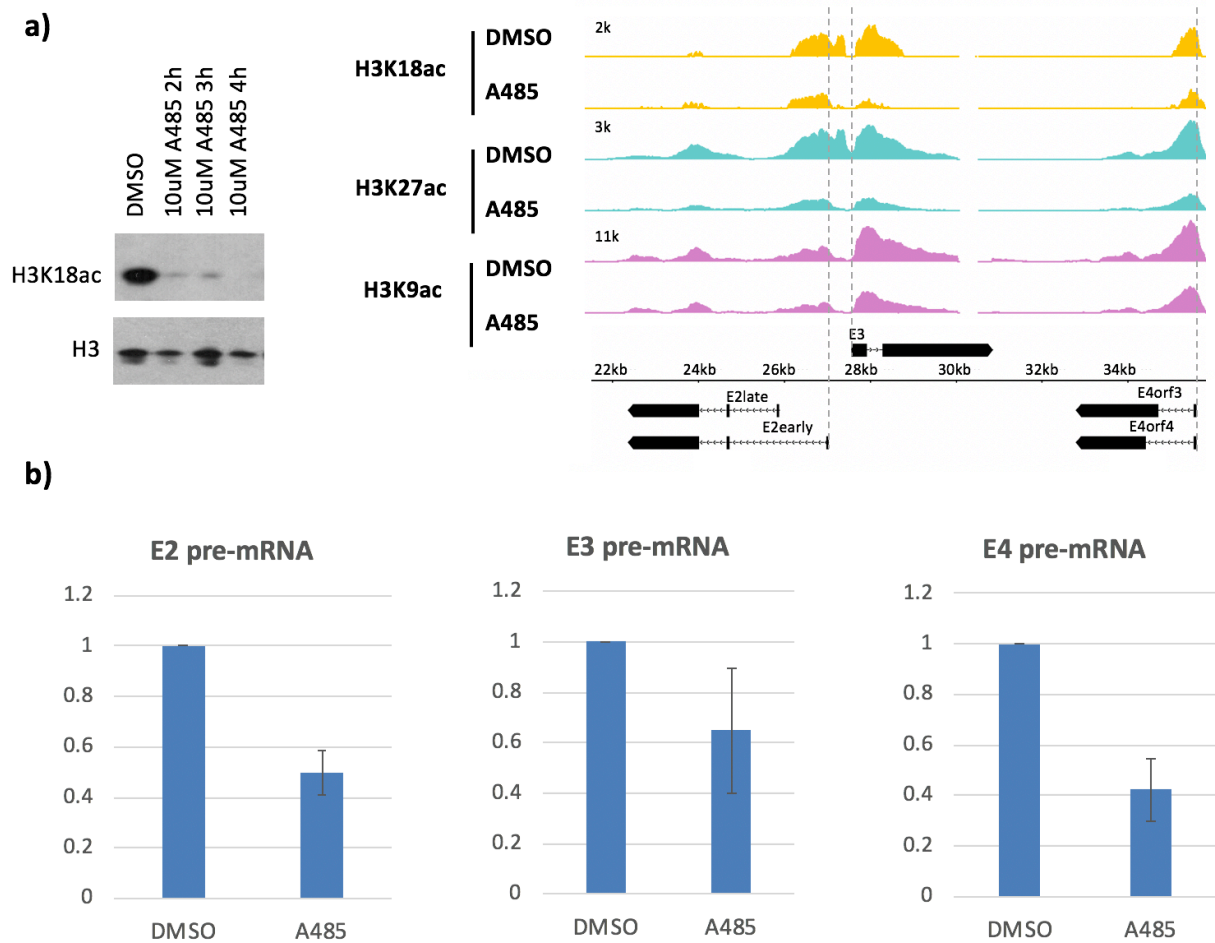
Figure 3-3: p300 HAT inhibitor A485 causes H3 hypoacetylation and decreased early viral gene expression

(a) (Left) Western blot showing H3K18ac and total H3 in HBTECs treated with 10uM A485 after 2, 3, or 4 hours. (Right) H3K18ac, H3K27ac, and H3K9ac ChIP-Seq at early viral promoters in cells treated with 10uM A485 for 2 hours.

(b) qRT-PCR for E2early, E3, and E4 pre-mRNA transcripts in cells treated with 10uM A485 for 2 hours.
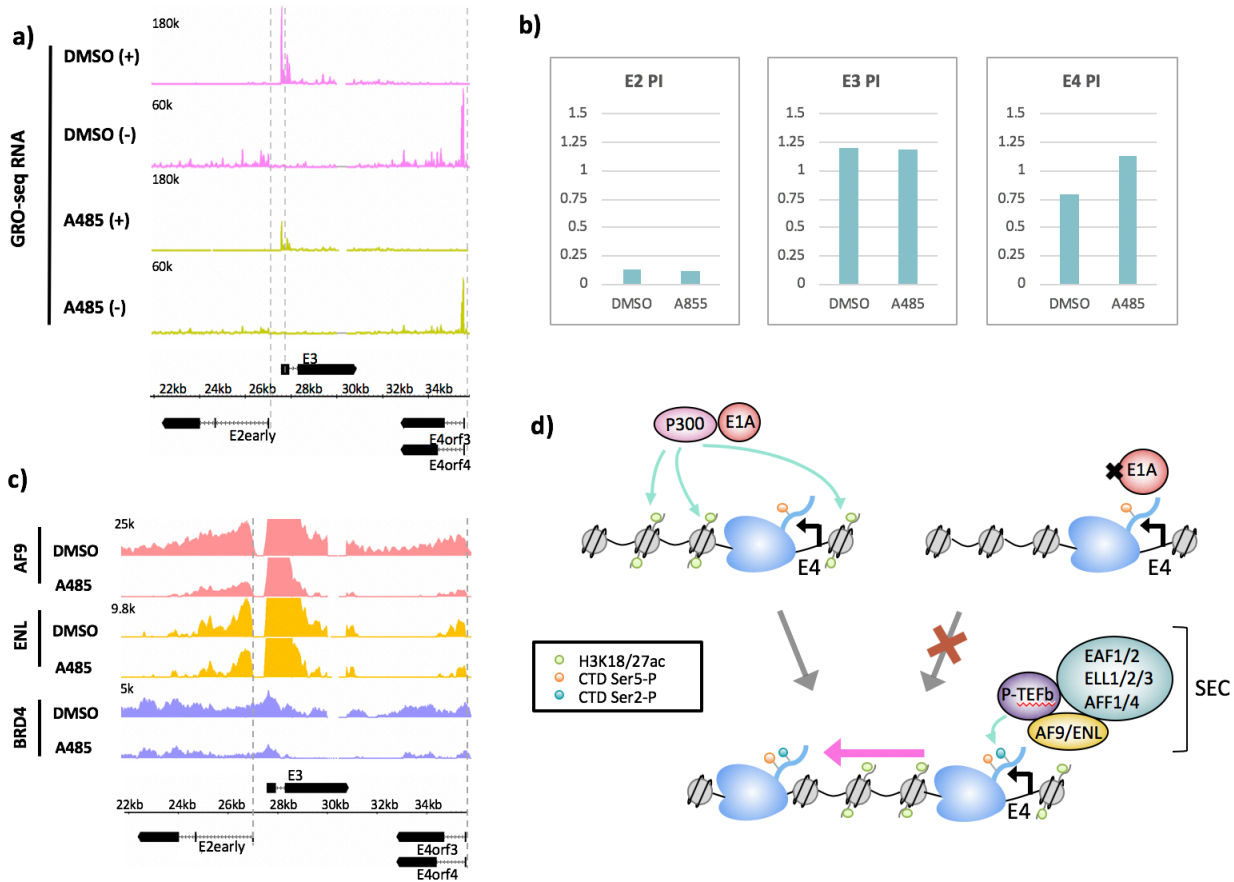
Figure 3-4: p300 HAT inhibition by A485 results in defective Pol2 pause release and decreased SEC and BRD4 binding at E4.

(a) GRO-seq in cells expressing wt E1A treated with DMSO or A485. Only the minus (-) strands are shown, which include the E2early and E4 transcripts. The data is shown twice, on two different y-axes.

(b) Pause indexes for E3 and E4 in cells treated with DMSO vs. A485.

(c) ChIP-seq for AF9, ENL, and BRD4 in cells treated with DMSO vs. A485.

(d) Model for regulation of E4 elongation by SEC binding to p300-E1A mediated H3K18/27ac .

P300 HAT inhibition by A485 differentially affects H3 acetylation at promoters and enhancers

In order to see if the effects of H3K18/27ac on Pol2 pause release at E4 is a general mechanism, we shifted our study to the human genome. First, we characterized the changes in H3K18/27ac in HBTECs after 2h treatment with 10uM A485. Western blotting with histones extracted from cells treated with A485 demonstrated a global decrease in H3K18ac (Figure 3-3a). Although H3K27ac is commonly used as a mark for active enhancers, it is also present at active promoters. Therefore, we used ChIP-seq for H3K18ac and H3K27ac to plot the average signals for these marks near all TSSs and at enhancer peaks (Figure 3-5a). We observed the expected decreases in H3K18ac and H3K27ac by A485 at enhancer peaks. However, we saw a surprising increase in H3K18ac and H3K27ac at TSSs in cells treated with A485.

We were also curious whether A485 treatment affected human genes during both initiation and elongation, similar to what occurs the ad5 genome. GRO-seq after A485 treatment was aligned to the human genome to determine what fraction of genes was affected by A485 at each stage in transcription. We limited ourselves to protein coding transcription units with at least 20 counts in the promoter region (TSS to +200) and a significant H3K9ac TSS peak, q-value <0.05. We found 1302 transcripts with defective initiation by A485 (>2-fold decrease in counts in the promoter region) and 993 transcripts with defective pause release by A485 (>2-fold increase in PI). There were 238 transcripts which passed the criteria for both groups (Figure 3-5b).

Hypoacetylation at TSSs and decreased SEC recruitment at genes with defective pol2 pause release with A485

Using the subset of transcripts with 2-fold increased PIs (referred to as "2XPI genes"), we plotted the average H3K18ac, H3K27ac, H3K9ac near TSSs in cells treated with DMSO or A485 (Figure 3-6a). In contrast to the increase in H3K18/27ac across all genes, H3K18/27ac at TSSs was decreased with A485 in 2XPI genes. H3K9ac, which didn't change at TSSs across all genes, also decreased at TSSs at 2XPI genes with A485 treatment. To determine if these decreases in H3 acetylation at 2XPI genes are correlated with decreased SEC component binding, we plotted AF9 and ENL in all genes and in 2XPI genes after A485 treatment (Figure 3-6b). Interestingly, AF9 and ENL were significantly higher at TSSs and in gene bodies of 2XPI genes, and decreased to the level of all genes after A485 treatment. BRD4, which was enriched at TSSs, was increased across all genes and slightly decreased in 2XPI genes after A485 treatment.

H3K9ac is sufficient for BRD4 enhancer binding which stimulates pausing at nearby genes

It was evident that BRD4 peaks were enriched at enhancers. Out of 26,534 BRD4 peaks, 14,877 (or 56%) were >2.5kb from the nearest TSS in cells treated with DMSO. Of these distal peaks, 84% overlapped with H3K27ac peaks, indicating enhancer binding. We clustered enhancer peaks based on whether BRD4 binding decreased with A485 treatment. There were 7554 peaks where BRD4 decreased >2-fold with A485 ("A485 sensitive"; Figure 3-7a, bottom) and 6324 peaks which did not ("A485 resistant"; Figure 3-7a, top). While A485 resistant peaks only correlated with decreased H3K18ac and H3K27ac, A485 sensitive peaks correlated with decreased H3K18ac, H3K27ac, and H3K9ac. This demonstrates that H3K9ac is sufficient for BRD4 enhancer binding.

We next asked if BRD4 enhancer binding affected pause release at nearby genes. We compared the difference in PI after A485 treatment at all genes to the difference in PI after A485

treatment at genes near decreased BRD4 peaks. There was a significant increase in PIs at genes

near decreased BRD4 peaks compared to all genes. These results indicate that H3K9ac is

sufficient for BRD4 enhancer binding, which stimulates pause release at nearby genes.
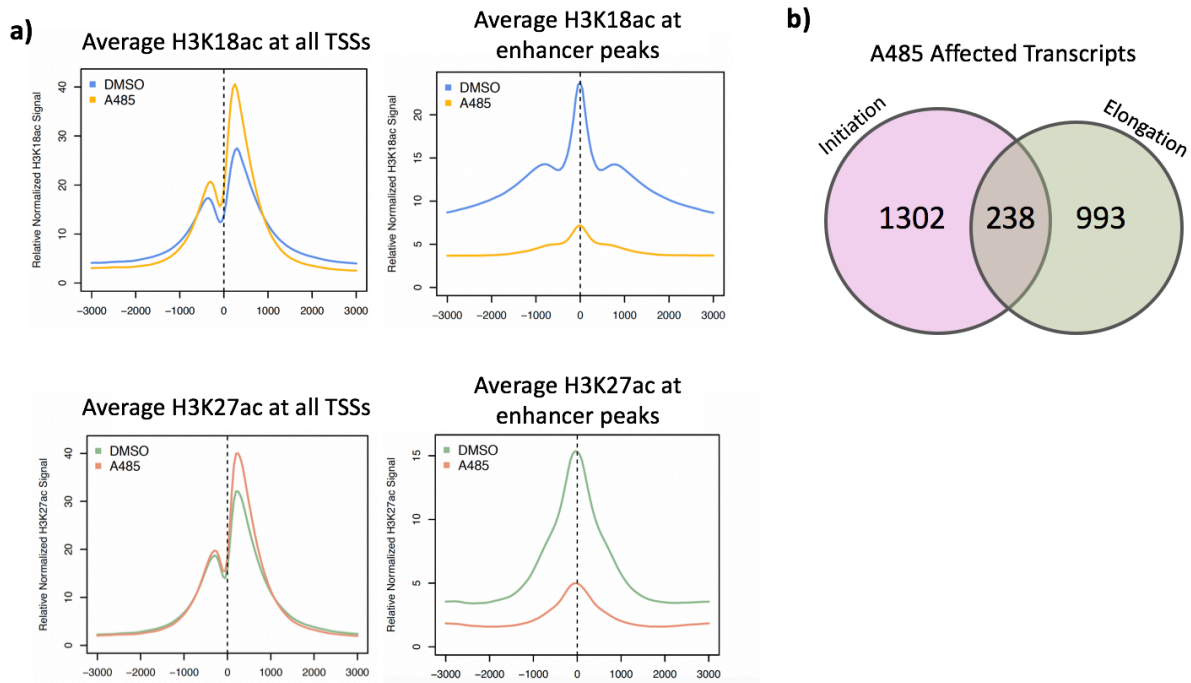
Figure 3- 5: Treatment with A485 causes different effects on acetylation at promoters vs. enhancers and effects both initiation and elongation

(a) Plots of average H3K18ac and H3K27ac signal at all TSSs and at enhancer peaks.

(b) Number of protein coding transcripts affected by A485 during initiation (>2-fold decrease in counts in the promoter region) and elongation (>2-fold increase in PI).
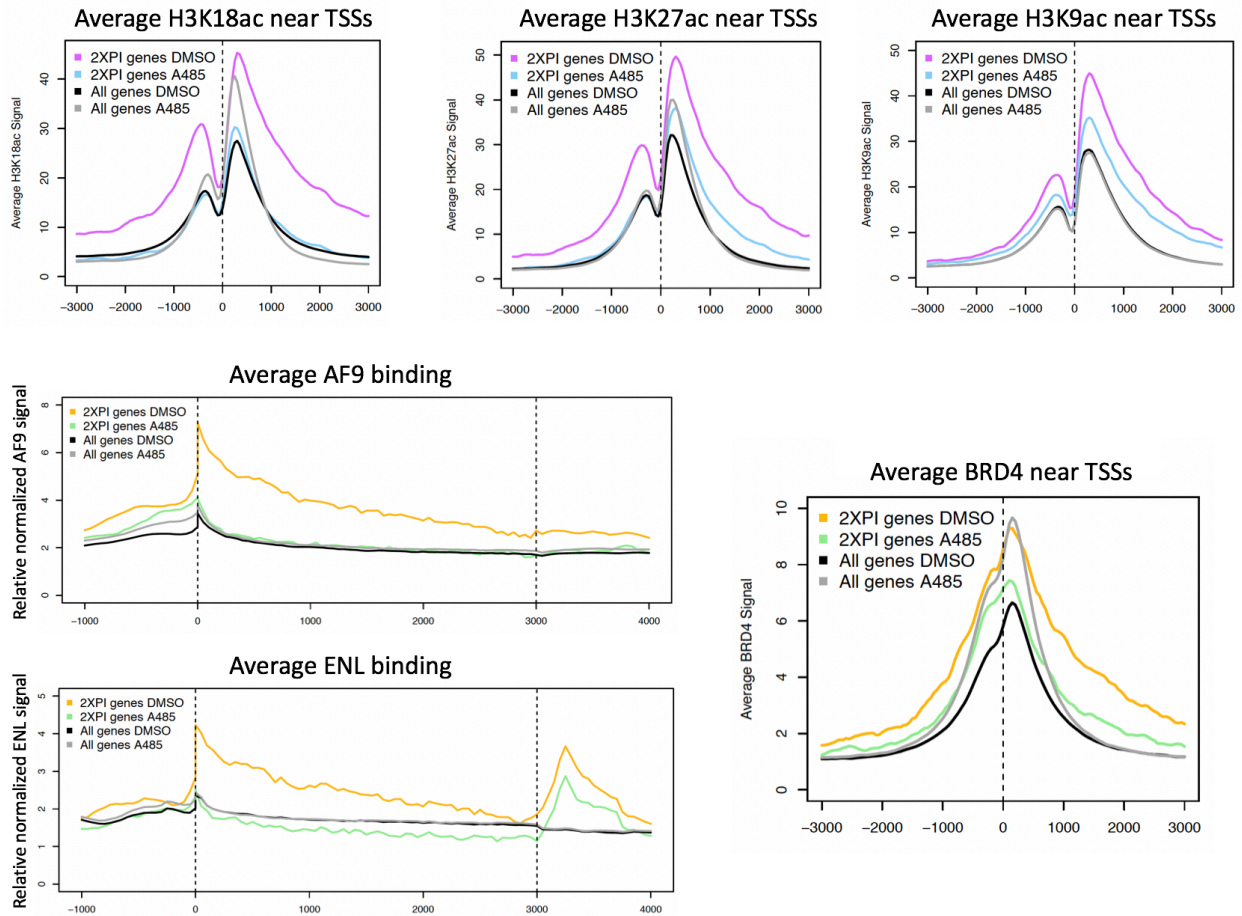
Figure 3-6: Paused genes affected by A485 are hypoacetylated at TSSs and have greatly increased SEC subunit binding

(a) Average H3K18ac, H3K27ac, and H3K9ac near TSSs in all genes and 2XPI genes after DMSO or A485 treatment.

(b) Average AF9 and ENL at all genes and 2XPI genes after DMSO or A485 treatment.

(c) Average BRD4 near TSSs in all genes and 2XPI genes after DMSO or A485 treatment.
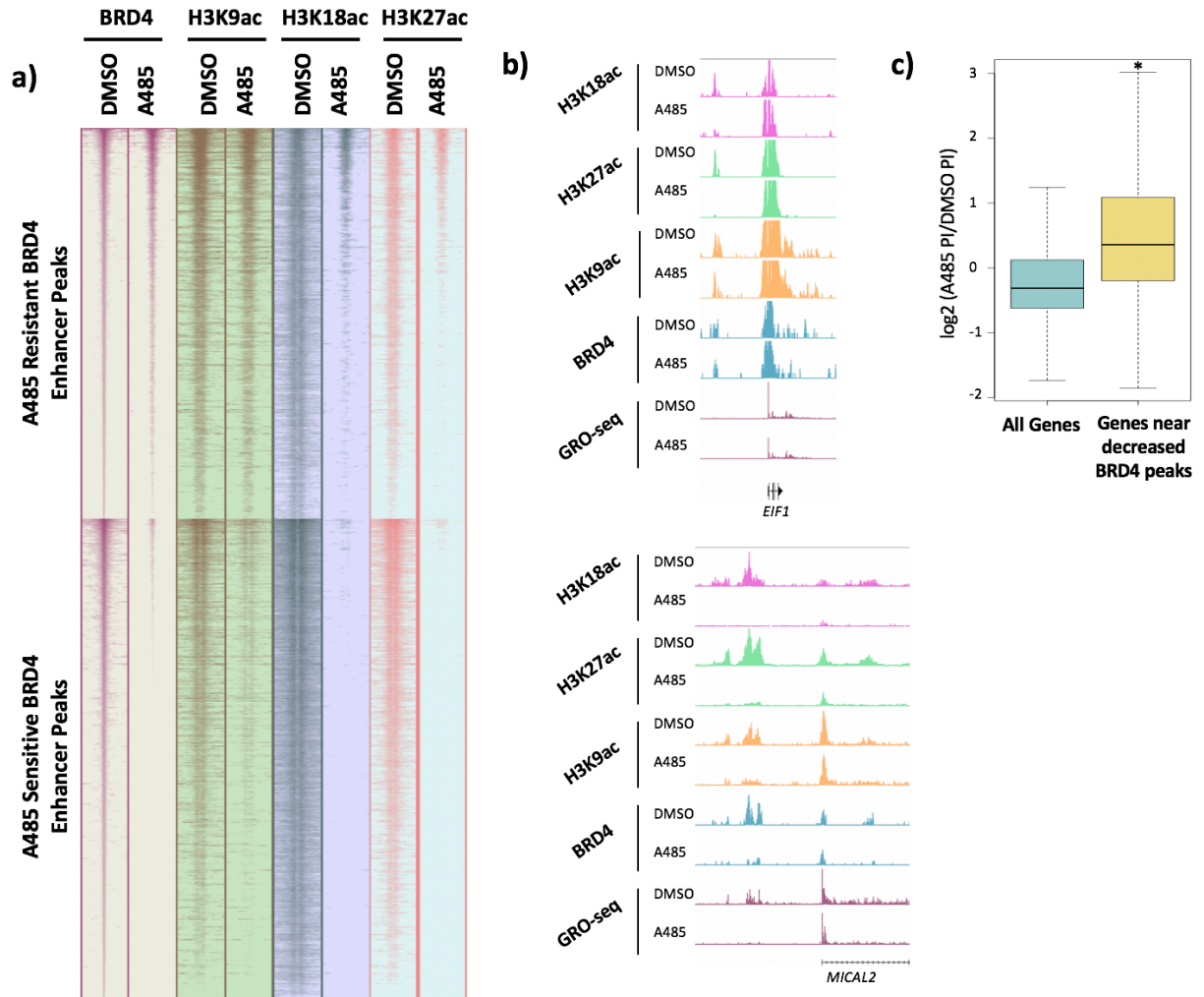
Figure 3-7: BRD4 enhancer binding stimulates pause release at nearby genes

(a) Heatmaps with BRD4, H3K9ac, H3K18ac, and H3K27ac ChIP-seq. BRD4 enhancer peaks which are A485 resistant (top cluster) and A485 sensitive (bottom cluster) are shown.

(b) Individual genes with A485 resistant (top) and A485 sensitive (bottom) BRD4 enhancer peaks plotted with H3K9ac, H3K18ac, and H3K27ac ChIP-seq, and GRO-seq.

(c) Boxplots comparing the change in PI after A485 treatment (log2 (A485 PI/DMSO PI)) in all genes vs. genes near decreased BRD4 peaks

Discussion

There is now a substantial base of knowledge which establishes correlation between histone N-terminal tail lysine acetylation and transcriptional activity. However, the mechanisms by which histone acetylation affects each step of transcription remains unclear. Our results present a mechanism which establishes causality between H3 acetylation and regulation during transcriptional elongation.

We propose a model in which SEC recruitment through the recognition of H3K18/27ac stimulates paused Pol2 release at E4. To do this, we used a previously described a large E1A p300-binding mutant (DM E1A) which causes decreased H3K18/27ac at the early adenoviral promoters E2early, E3, and E4. GRO-seq was performed in cells expressing wt E1A vs. DM E1A in order to determine the effects of p300 recruitment by E1A and resultant H3K18/27ac on Pol2 pause release on the Ad5 genome. With DM E1A, the pausing index at E4 increased almost 2-fold, demonstrating that H3K18/27ac contributes to paused Pol2 release at E4.

We found a correlation between defective paused Pol2 release and decreased binding of SEC components CDK9, AF9, and ENL, indicating that H3K18/27ac is necessary for maximal SEC recruitment and efficient pause release. This is similar to a role of H3K9ac, which acts as a substrate for AF9 and ENL and promotes paused Pol2 release by directly recruiting the SEC (60). While SEC recruitment by H3K18/27ac may be due to recruitment of YEATS domains present in AF9 and ENL, other components may also be responsible. For example, the SEC has been shown to be recruited to H3K27ac through the C-terminus of the central scaffold protein AFF4 at the TSS of the ESR1 gene in breast cancer cells (70).

The inhibitory effects of H3K18/27 hypoacetylation on pause release and SEC recruitment at E4 were recapitulated in cells treated with the p300 HAT inhibitor A485. While

this does not rule out the possibility of interactions between p300 and other co-activators, such as the demonstrated recruitment of other chromatin modifying proteins (71, 72), it does demonstrate that the HAT activity itself is essential for maximal pause release at E4. Analysis of these data sets on the human genome establish this as a general mechanism. We observed the expected decrease in H3K18/27ac at enhancers, along with an intriguing increase at TSSs of all genes, which hints towards differential dynamics of HAT and HDAC activities at promoters vs. enhancers, a general phenomenon which has been shown on a subset of genes (73). A485 results in defects in pause release in a large number of human genes (2XPI genes) which also share distinct signatures of H3 acetylation at TSSs and SEC subunit binding. These genes are unique in that acetylation was decreased at TSSs with A485 treatment, with the greatest decrease occurring in H3K18ac, suggesting the importance of this mark in SEC recognition.

BRD4 contains two bromodomains, which interact with acetylated histones (74, 75). Through its C-terminal tail, it interacts with P-TEFb and is thought to recruit it to hyperacetylated genomic regions (76). It has been shown to bind to promoters and enhancers, and to act as a histone chaperone by facilitating elongation of both protein coding and enhancer RNAs (54). We found a subset of BRD4 enhancer peaks which were decreased after treatment with the CBP/p300 HAT inhibitor A485, in contrast to the average increased BRD4 signal at TSSs with A485. This presented an opportunity to study the effects of BRD4 enhancer binding on elongation. Interestingly, we found that H3K9ac is sufficient for BRD4 recruitment at enhancers. Additionally, GRO-seq in cells treated with A485 revealed a correlation between decreased BRD4 peaks and defective release of paused pol2. The mechanism by which this occurs is likely by recruitment of BRD4 to enhancers, which make contact with promoters through Mediator binding (77). Another possibility is that transcription of enhancer RNAs

stimulated by BRD4 affect stimulates paused Pol2 release elongation by promoting NELF

release (78).

Taken together, our results present an interesting causal link between H3 acetylation and

paused Pol2 release by SEC and BRD4 recruitment. Regulation of elongation by the SEC has

several interesting implications for disease. SEC proteins are common translocation partners of

mixed lineage leukemia (MLL), which contribute to myeloid and lymphoblastic leukemia

pathogenesis. Important roles for regulation of SEC assembly have also been shown for HIV and

MYC-dependent cancer.

Chapter 4: MATERIALS AND METHODS

Plasmids

The plasmids used for *in vivo* colocalization assays and luciferase reporter transient-transfection assays were constructed from plasmid NYE127 (29) containing the F9-polyomavirus early promoter driving expression of the SV40 T-antigen nuclear localization sequence (NLS)-EYFP-lac repressor fusion fused to fragments of large E1A [e.g., NLS-EYFP-LacI-E1A(aa 121–223)] (27). The five C-terminal amino acids of LacI are deleted in these expression vectors so that the fusion proteins form LacI dimers, not tetramers (26). PCR amplification of regions encoding the indicated large E1A amino acids were cloned into the NYE127 derivatives via a SacI restriction site and verified by sequencing. For cyan fluorescent protein (CFP) or mCherry-labeled proteins, enhanced yellow fluorescent protein (EYFP) was replaced by ECFP or mCherry generated by PCR and confirmed by sequencing.

Confocal microscopy of transfected CHO-A03.1 cells

CHO-A03.1 cells (26)were plated on fibronectin-coated 6-well plates and transfected using Lipofectamine 2000 (Invitrogen) with 2 μg of expression vector for LacI-CFP-E1A or LacI-mCherry-E1A and 2 μg of expression vector for YFP-MED6, YFP-MED23, or YFP-p300 (6, 27). After 48 h, cells were fixed in 2% paraformaldehyde, washed in 1× phosphate-buffered saline (PBS), and stained with 4′,6-diamidino-2-phenylindole (DAPI) in 0.05% Triton X-100 in PBS for 20 min. Cells were mounted onto slides and imaged for colocalization of CFP or mCherry and YFP using a Leica TCS SP2 AOBS single-photon confocal microscope using a 63×, 1.4-numerical-aperture oil immersion objective.

Transient-transfection reporter assays

Transfection was done into CHO-K1 cells, the parental cell for A03.1 cells used in the

fluorescence microscopy colocalization assay (26). Seventy percent confluent 12-well culture

plates were transfected with 100 ng expression vectors for NLS-mCherry-LacI fused to the

indicated fragments of large E1A (Figure 2-2a), 300 ng NYE107b luciferase reporter plasmid

with eight *lacO* sites upstream of the Ad2 E1B promoter driving firefly luciferase expression

(29), and 300 ng pRL-TK (Promega) per well. Cells were cultured for 24 h, extracts were

prepared and assayed for firefly and Renilla luciferase activity using the Promega Dual-

Luciferase assay kit, and firefly luciferase activity was normalized to Renilla luciferase activity.

Construction of Ad5 mutants

The wt Ad2 sequence from aa 1 to 3153 was cloned between the SfII site next to Ad5 nucleotide

1 and the StuI site at Ad5 nucleotide 3153 in plasmid pAdlox (30). Oligonucleotide-directed

mutagenesis was used to substitute alanine codons for wt Ad2 E1A codons, as shown in Figure

2-2g. The resulting plasmids were cut with SfiI and cotransfected into 293-CRE cells with Ψ5

DNA (30). Cre-mediated recombination between the *loxP* site in Ψ5 at base pair 3201 and

the *loxP* site in the plasmids derived from pAdlox with the engineered E1A mutations generates

genomes with inverted terminal repeats and the left end packaging sequences capable of

replicating and being packaged into virions in 293 cells (30). In addition to the engineered E1A

mutations, all of these mutants have a substitution in E3 (30) and an out-of-frame insertion of

a *loxP* site near the C-terminal end of the E1B-55K coding region that probably inactivates E1B-

55K function (79). The virus expressing wt E1A in these studies was constructed in the same

way using a pAdlox plasmid with wt Ad2 E1A sequence.

Cell culture

Human bronchial/tracheal epithelial cells (HBTEC; catalog number FC-0035, lot number 02196; Lifeline Cell Technology) were grown at 37°C in a BronchiaLife medium complete kit (LL-0023; Lifeline Cell Technology) in a 5% CO2 incubator until they reached confluence. Cells were then incubated 3 days more without addition of fresh medium and were infected with the indicated Ad mutants under the conditioned medium.

qRT-PCR

Total RNA extracted from HTBECs using a PureLink RNA minikit (Ambion) was reverse transcribed with random hexamer priming using Superscript III (Invitrogen). RNA was treated with DNase I with a DNA-free kit (Ambion). Quantitative reverse transcription-PCRs (qRT-PCRs) were carried out with the Applied Biosystems 7500 real-time PCR system with FastStart universal SYBR green master mix (Roche). All values were normalized to 18S RNA levels.

ChIP-seq

Preparation of cross-linked HBTEC chromatin, sonication, and immunoprecipitation was as described in Ferrari et al., 2014 (6). Sequencing libraries were constructed from 1 ng of immunoprecipitated and input DNA using the KAPA Hyper Prep kit (KAPA Biosystems) and NEXTflex ChIP-seq barcodes (Bio Scientific). Sequence tags were aligned to the Ad5 genome and normalized to the following formula: (number of Ad5-aligned reads in the input sample/number of human-aligned reads in the input sample) × (number of Ad5-aligned reads in the ChIP sample).

GRO-seq

GRO-seq experiments were performed as described by Core et al. (62).

Antibodies

Antibodies included H3K9ac (07-352; Millipore) and H3K18ac (814), prepared and validated as described previously (80), as well as H3K27ac (39133; Active Motif), Pol2 8WG16 (sc-56767; Santa Cruz), TBP (C15200002; Diagenode), anti-e1a MAb M73 (81), Ku-86 H-300 (sc-9034; Santa Cruz), ENL (14893S, Cell Signaling), AF9 (GTX102835, Genetex), BRD4 (A301-985A50), NELF TH1L D5G6W (12265S Cell Signaling), Pol2 Ser2-P 31Z3G (13499, Cell Signaling), Pol2 Ser5-P D9N5I (13523, Cell Signaling) , and CDK9 C12F7 (2316, Cell Signaling).

Chapter 5: CONCLUDING REMARKS

Despite a wealth of data associating promoter and enhancer region histone N-terminal tail lysine acetylation with transcriptional activity, there are relatively few examples of studies that establish causation between these histone posttranslational modifications and transcription. While hypoacetylation of histone H3K18/27 is associated with repression, the step(s) in the overall process of transcription that is blocked at a hypoacetylated promoter is not clearly established in most instances. Studies presented here provide detailed models of how H3K18/27ac is linked to transcriptional initiation and elongation.

REFERENCES

1.   Pelka P, Ablack JNG, Torchia J, Turnell AS, Grand RJA, Mymryk JS. 2009.

Transcriptional control by adenovirus E1A conserved region 3 via p300/CBP. Nucleic

Acids Res 37:1095–1106.

2.   Zhao H, Chen M, Pettersson U. 2014. A new look at adenovirus splicing. Virology 456–

457:329–341.

3.   Perricaudet M, Akusjärvi G, Virtanen A, Pettersson U. 1979. Structure of two spliced

mRNAs from the transforming region of human subgroup C adenoviruses. Nature

281:694–696.

4.   Avvakumov N, Kajon AE, Hoeben RC, Mymryk JS. 2004. Comprehensive sequence

analysis of the E1A proteins of human and simian adenoviruses. Virology 329:477–492.

5.   Kimelman D, Miller JS, Porter D, Roberts BE. 1985. E1a regions of the human

adenoviruses and of the highly oncogenic simian adenovirus 7 are closely related. J Virol

53:399–409.

6.   Ferrari R, Gou D, Jawdekar G, Johnson SA, Nava M, Su T, Yousef AF, Zemke NR,

Pellegrini M, Kurdistani SK, Berk AJ. 2014. Adenovirus small E1A employs the lysine

acetylases p300/CBP and tumor suppressor RB to repress select host genes and promote

productive virus infection. Cell Host Microbe 16:663–676.

7.   Pelka P, Ablack JNG, Fonseca GJ, Yousef AF, Mymryk JS. 2008. Intrinsic Structural

Disorder in Adenovirus E1A: a Viral Molecular Hub Linking Multiple Diverse Processes.

J Virol 82:7252–7263.

8.   Ferreon JC, Martinez-Yamout MA, Dyson HJ, Wright PE. 2009. Structural basis for

subversion of cellular control mechanisms by the adenoviral E1A oncoprotein. Proc Natl Acad Sci U S A 106:13260–13265.

9. Horwitz GA, Zhang K, McBrian MA, Grunstein M, Kurdistani SK, Berk AJ. 2008. Adenovirus small e1a alters global patterns of histone modification. Science (80-) 321:1084–1085.

10. Jin Q, Yu L-R, Wang L, Zhang Z, Kasper LH, Lee J-E, Wang C, Brindle PK, Dent SYR, Ge K. 2011. Distinct roles of GCN5/PCAF-mediated H3K9ac and CBP/p300-mediated H3K18/27ac in nuclear receptor transactivation. EMBO J 30:249–62.

11. Berk AJ, Lee F, Harrison T, Williams J, Sharp PA. 1979. Pre-early adenovirus 5 gene product regulates synthesis of early viral messenger RNAs. Cell 17:935–944.

12. Jones N, Shenk T. 1979. Isolation of adenovirus type 5 host range deletion mutants defective for transformation of rat embryo cells. Cell 17:683–689.

13. Montell C, Courtois G, Eng C, Berk A. 1984. Complete transformation by adenovirus 2 requires both E1A proteins. Cell 36:951–961.

14. Winberg G, Shenk T. 1984. Dissection of overlapping functions within the adenovirus type 5 E1A gene. EMBO J 3:1907–12.

15. Lillie JW, Green MR. 1989. Transcription activation by the adenovirus E1a protein. Nature.

16. Martin KJ, Lillie JW, Green MR. 1990. Evidence for interaction of different eukaryotic transcriptional activators with distinct cellular targets. Nature 346:147–152.

17. Bondesson M, Svensson C, Linder S, Akusjärvi G. 1992. The carboxy-terminal exon of the adenovirus E1A protein is required for E4F-dependent transcription activation. EMBO J 11:3347–3354.

18. Ström a C, Ohlsson P, Akusjärvi G. 1998. AR1 is an integral part of the adenovirus type 2 E1A-CR3 transactivation domain. J Virol 72:5978–83.

19. Webster LC, Ricciardi RP. 1991. trans-dominant mutants of E1A provide genetic evidence that the zinc finger of the trans-activating domain binds a transcription factor. Mol Cell Biol 11:4287–4296.

20. Liu F, Green MR. 1994. Promoter targeting by adenovirus E1a through interaction with different cellular DNA-binding domains. Nature 368:520–525.

21. Boyer TG, Martin ME, Lees E, Ricciardi RP, Berk AJ. 1999. Mammalian Srb/Mediator complex is targeted by adenovirus E1A protein. Nature 399:276–279.

22. Malik S, Roeder RG. 2010. The metazoan Mediator co-activator complex as an integrative hub for transcriptional regulation. Nat Rev Genet 11:761–772.

23. Tsai KL, Tomomori-Sato C, Sato S, Conaway RC, Conaway JW, Asturias FJ. 2014. Subunit architecture and functional modular rearrangements of the transcriptional mediator complex. Cell 157:1430–1444.

24. Wang G, Berk AJ. 2002. In vivo association of adenovirus large E1A protein with the human mediator complex in adenovirus-infected and -transformed cells. J Virol 76:9186–9193.

25. Cantin GT, Stevens JL, Berk AJ. 2003. Activation domain-mediator interactions promote transcription preinitiation complex assembly on promoter DNA. Proc Natl Acad Sci U S A 100:12003–8.

26. Tumbar T, Sudlow G, Belmont AS. 1999. Large-scale chromatin unfolding and remodeling induced by VP16 acidic activation domain. J Cell Biol 145:1341–1354.

27. Balamotis M a, Pennella M a, Stevens JL, Wasylyk B, Belmont AS, Berk AJ. 2009.

Complexity in transcription control at the activation domain-mediator interface. Sci Signal 2:ra20.

28.   Culp JS, Webster LC, Friedman DJ, Smith CL, Huang WJ, Wu FY, Rosenberg M, Ricciardi RP. 1988. The 289-amino acid E1A protein of adenovirus binds zinc in a region that is important for trans-activation. Proc Natl Acad Sci U S A 85:6450–4.

29.   Carpenter AE, Ashouri A, Belmont AS. 2004. Automated microscopy identifies estrogen receptor subdomains with large-scale chromatin structure unfolding activity. Cytometry A 58:157–66.

30.   Hardy S, Kitamura M, Harris-Stansil T, Dai Y, Phipps ML. 1997. Construction of adenovirus vectors through Cre-lox recombination. J Virol 71:1842–1849.

31.   Roberts RJ, Sciaky D, Gelinas RE, Jiang B, Yen CE, Kelly MM, Bullock PA, Parsons BL, Neill KEO, Gingeras TR. 1981. Information Content of the Adenovirus-2 Genome 2.

32.   Spector DJ, Parks CL, Knittle RA. 1993. A multicomponent cis-activator of transcription of the e1b gene of adenovirus type 5. Virology 194:128–136.

33.   Maxfield LF, Spector DJ. 1997. Readthrough activation of early adenovirus E1b gene transcription. J Virol 71:8321–9.

34.   Horwitz GA, Zhang K, McBrian MA, Grunstein M, Kurdistani SK, Berk AJ. 2008. Adenovirus Small e1a Alters Global Patterns of Histone Modification. Science (80-) 321:1084–1085.

35.   Maze I, Noh KM, Allis CD. 2013. Histone regulation in the CNS: Basic principles of epigenetic plasticity. Neuropsychopharmacology.

36.   Jiang C, Pugh BF. 2009. Nucleosome positioning and gene regulation: advances through genomics. Nat Rev Genet 10:161–172.

37.   Sainsbury S, Bernecky C, Cramer P. 2015. Structural basis of transcription initiation by RNA polymerase II. Nat Rev Mol Cell Biol 16:129–143.

38.   Soshnev AA, Josefowicz SZ, Allis CD. 2016. Greater Than the Sum of Parts: Complexity of the Dynamic Epigenome. Mol Cell.

39.   Avvakumov N, Kajon AE, Hoeben RC, Mymryk JS. 2004. Comprehensive sequence analysis of the E1A proteins of human and simian adenoviruses. Virology 329:477–492.

40.   Stevens JL. 2002. Transcription Control by E1A and MAP Kinase Pathway via Sur2 Mediator Subunit. Science (80-) 296:755–758.

41.   Fang L, Stevens JL, Berk AJ, Spindler KR. 2004. Requirement of Sur2 for efficient replication of mouse adenovirus type 1. J Virol 78:12888–12900.

42.   Mittler G, Stühler T, Santolin L, Uhlmann T, Kremmer E, Lottspeich F, Berti L, Meisterernst M. 2003. A novel docking site on Mediator is critical for activation by VP16 in mammalian cells. EMBO J 22:6494–6504.

43.   Vojnic E, Mourão A, Seizl M, Simon B, Wenzeck L, Larivière L, Baumli S, Baumgart K, Meisterernst M, Sattler M, Cramer P. 2011. Structure and VP16 binding of the Mediator Med25 activator interaction domain. Nat Struct Mol Biol 18:404–409.

44.   Bernecky C, Taatjes DJ. 2012. Activator-mediator binding stabilizes RNA polymerase II orientation within the human mediator-RNA polymerase II-TFIIF assembly. J Mol Biol 417:387–394.

45.   Meyer KD, Lin S-C, Bernecky C, Gao Y, Taatjes DJ. 2010. p53 activates transcription by directing structural shifts in Mediator. Nat Struct Mol Biol 17:753–60.

46.   Leong K, Lee W, Berk AJ. 1990. High-level transcription from the adenovirus major late promoter requires downstream binding sites for late-phase-specific factors. J Virol 64:51–

60.

47.   Kassavetis GA, Braun BR, Nguyen LH, Peter Geiduschek E. 1990. S. cerevisiae TFIIIB is
        the transcription initiation factor proper of RNA polymerase III, while TFIIIA and TFIIIC
        are assembly factors. Cell 60:235–245.

48.   Cai H, Luse DS. 1987. Transcription initiation by RNA polymerase II in vitro. Properties
        of preinitiation, initiation, and elongation complexes. J Biol Chem 262:298–304.

49.   Juo ZS, Kassavetis GA, Wang J, Geiduschek EP, Sigler PB. 2003. Crystal structure of a
        transcription factor IIIB core interface ternary complex. Nature 422:534–539.

50.   Ferri E, Petosa C, McKenna CE. 2016. Bromodomains: Structure, function and
        pharmacology of inhibition. Biochem Pharmacol.

51.   Fonseca GJ, Cohen MJ, Mymryk JS. 2014. Adenovirus E1A Recruits the Human Paf1
        Complex To Enhance Transcriptional Elongation. J Virol 88:5630–5637.

52.   Jonkers I, Lis JT. 2015. Getting up to speed with transcription elongation by RNA
        polymerase II. Nat Rev Mol Cell Biol.

53.   Adelman K, Lis JT. 2012. Promoter-proximal pausing of RNA polymerase II: emerging
        roles in metazoans. Nat Rev Genet 13:720–731.

54.   Kanno T, Kanno Y, Leroy G, Campos E, Sun HW, Brooks SR, Vahedi G, Heightman TD,
        Garcia BA, Reinberg D, Siebenlist U, O'Shea JJ, Ozato K. 2014. BRD4 assists elongation
        of both coding and enhancer RNAs by interacting with acetylated histones. Nat Struct Mol
        Biol 21:1047–1057.

55.   Boija A, Mahat DB, Zare A, Holmqvist PH, Philip P, Meyers DJ, Cole PA, Lis JT,
        Stenberg P, Mannervik M. 2017. CBP Regulates Recruitment and Release of Promoter-
        Proximal RNA Polymerase II. Mol Cell 68:491–503.e5.

56.   Pathak R, Singh P, Ananthakrishnan S, Adamczyk S, Schimmel O, Govind CK. 2018. Acetylation-Dependent Recruitment of the FACT Complex and Its Role in Regulating Pol II Occupancy Genome-Wide in *Saccharomyces cerevisiae*. Genetics genetics.300943.2018.

57.   Luo Z, Lin C, Shilatifard A. 2012. The super elongation complex (SEC) family in transcriptional control. Nat Rev Mol Cell Biol 13:543–547.

58.   He N, Chan CK, Sobhian B, Chou S, Xue Y, Liu M, Alber T, Benkirane M, Zhou Q. 2011. Human Polymerase-Associated Factor complex (PAFc) connects the Super Elongation Complex (SEC) to RNA polymerase II on chromatin. Proc Natl Acad Sci U S A 108.

59.   Li Y, Wen H, Xi Y, Tanaka K, Wang H, Peng D, Ren Y, Jin Q, Dent SYR, Li W, Li H, Shi X. 2014. AF9 YEATS domain links histone acetylation to DOT1L-mediated H3K79 methylation. Cell 159:558–571.

60.   Gates LA, Shi J, Rohira AD, Feng Q, Zhu B, Bedford MT, Sagum CA, Jung SY, Qin J, Tsai MJ, Tsai SY, Li W, Foulds CE, O'Malley BW. 2017. Acetylation on histone H3 lysine 9 mediates a switch from transcription initiation to elongation. J Biol Chem 292:14456–14472.

61.   Hsu E, Pennella MA, Zemke NR, Eng C, Berk AJ. 2018. Adenovirus E1A Activation Domain Regulates H3 Acetylation Affecting Varied Steps in Transcription at Different Viral Promoters. J Virol 92.

62.   Core LJ, Waterfall JJ, Lis JT. 2008. Nascent RNA sequencing reveals widespread pausing and divergent initiation at human promoters. Science (80-) 322:1845–1848.

63.   Shukla S, Oberdoerffer S. 2012. Co-transcriptional regulation of alternative pre-mRNA

splicing. Biochim Biophys Acta 1819:673–683.

64.   Alexander RD, Innocente SA, Barrass JD, Beggs JD. 2010. Splicing-dependent RNA

        polymerase pausing in yeast. Mol Cell 40:582–593.

65.   Nguyen VT, Kiss T, Michels AA, Bensaude O. 2001. 7SK small nuclear RNA binds to

        and inhibits the activity of CDK9/cyclin T complexes. Nature 414:322–325.

66.   Yang Z, Zhu Q, Luo K, Zhou Q. 2001. The 7SK small nuclear RNA inhibits the

        CDK9/cyclin T1 kinase to control transcription. Nature 414:317–322.

67.   Li Q, Price JP, Byers SA, Cheng D, Peng J, Price DH. 2005. Analysis of the large inactive

        P-TEFb complex indicates that it contains one 7SK molecule, a dimer of HEXIM1 or

        HEXIM2, and two P-TEFb molecules containing Cdk9 phosphorylated at threonine 186. J

        Biol Chem 280:28819–28826.

68.   Chen FX, Smith ER, Shilatifard A. 2018. Born to run: control of transcription elongation

        by RNA polymerase II. Nat Rev Mol Cell Biol 19:464–478.

69.   Lasko LM, Jakob CG, Edalji RP, Qiu W, Montgomery D, Digiammarino EL, Hansen TM,

        Risi RM, Frey R, Manaves V, Shaw B, Algire M, Hessler P, Lam LT, Uziel T, Faivre E,

        Ferguson D, Buchanan FG, Martin RL, Torrent M, Chiang GG, Karukurichi K, Langston

        JW, Weinert BT, Choudhary C, de Vries P, Van Drie JH, McElligott D, Kesicki E,

        Marmorstein R, Sun C, Cole PA, Rosenberg SH, Michaelides MR, Lai A, Bromberg KD.

        2017. Discovery of a selective catalytic p300/CBP inhibitor that targets lineage-specific

        tumours. Nature2017/09/27. 550:128–132.

70.   Gao Y, Chen L, Han Y, Wu F, Yang W-S, Zhang Z, Huo T, Zhu Y, Yu C, Kim H, Lee M,

        Tang Z, Phillips K, He B, Jung SY, Song Y, Zhu B, Xu R-M, Feng Q. 2020. Acetylation

        of histone H3K27 signals the transcriptional elongation for estrogen receptor alpha.

Commun Biol 3:165.

71.   Vandel L, Trouche D. 2001. Physical association between the histone acetyl transferase CBP and a histone methyl transferase. EMBO Rep 2:21–26.

72.   Chan HM, La Thangue NB. 2001. p300/CBP proteins: HATs for transcriptional bridges and scaffolds. J Cell Sci 114:2363 LP-2373.

73.   Weinert BT, Narita T, Satpathy S, Srinivasan B, Hansen BK, Schölz C, Hamilton WB, Zucconi BE, Wang WW, Liu WR, Brickman JM, Kesicki EA, Lai A, Bromberg KD, Cole PA, Choudhary C. 2018. Time-Resolved Analysis Reveals Rapid Dynamics and Broad Scope of the CBP/p300 Acetylome. Cell2018/05/24. 174:231–244.e12.

74.   Filippakopoulos P, Picaud S, Mangos M, Keates T, Lambert J-P, Barsyte-Lovejoy D, Felletar I, Volkmer R, Müller S, Pawson T, Gingras A-C, Arrowsmith CH, Knapp S. 2012. Histone recognition and large-scale structural analysis of the human bromodomain family. Cell 149:214–231.

75.   Kanno T, Kanno Y, Siegel RM, Jang MK, Lenardo MJ, Ozato K. 2004. Selective recognition of acetylated histones by bromodomain proteins visualized in living cells. Mol Cell 13:33–43.

76.   Bisgrove DA, Mahmoudi T, Henklein P, Verdin E. 2007. Conserved P-TEFb-interacting domain of BRD4 inhibits HIV transcription. Proc Natl Acad Sci U S A 104:13690–13695.

77.   Takahashi H, Parmely TJ, Sato S, Tomomori-Sato C, Banks CAS, Kong SE, Szutorisz H, Swanson SK, Martin-Brown S, Washburn MP, Florens L, Seidel CW, Lin C, Smith ER, Shilatifard A, Conaway RC, Conaway JW. 2011. Human mediator subunit MED26 functions as a docking site for transcription elongation factors. Cell 146:92–104.

78.   Schaukowitch K, Joo J-Y, Liu X, Watts JK, Martinez C, Kim T-K. 2014. Enhancer RNA

facilitates NELF release from immediate early genes. Mol Cell 56:29–42.

79.   Yew PR, Cheng Kao C, Berk AJ. 1990. Dissection of functional domains in the
        adenovirus 2 early 1b 55k polypeptide by suppressor-linker insertional mutagenesis.
        Virology 179:795–805.

80.   Ferrari R, Su T, Li B, Bonora G, Oberai A, Chan Y, Sasidharan R, Berk AJ, Pellegrini M,
        Kurdistani SK. 2012. Reorganization of the host epigenome by a viral oncogene. Genome
        Res 22:1212–1221.

81.   Harlow E, Franza BR, Schley C. 1985. Monoclonal antibodies specific for adenovirus
        early region 1A proteins: extensive heterogeneity in early region 1A products. J Virol
        55:533–546.